ANNUAL REVIEWS

Annual Review of Marine Science

The Energetics of Fine-Scale Air–Sea Interactions

Lionel Renault,[1] Jacob O. Wenegrat,[2] Hyodae Seo,[3] and Patrick Marchesiello[1]

[1]Université de Toulouse, LEGOS (Laboratoire d'Etudes en Géophysique et Océanographie Spatiales), CNES/CNRS/IRD/UT3, Toulouse, France; email: lionel.renault@ird.fr

[2]Department of Atmospheric and Oceanic Science, University of Maryland, College Park, Maryland, USA

[3]Department of Oceanography, University of Hawai'i at Mānoa, Honolulu, Hawaii, USA

Annu. Rev. Mar. Sci. 2027. 19:3.1–3.27

The *Annual Review of Marine Science* is online at marine.annualreviews.org

https://doi.org/10.1146/annurev-marine-040425-024449

Keywords

fine-scale energetics, air–sea interactions, wave–wind feedback, large-scale effects, modeling, observations

Abstract

The Earth's oceanic energy cycle is a multiscale system governed by the complex interactions of oceanic, atmospheric, and wave processes. Significant progress has been made in understanding energy exchange at planetary scales. However, challenges remain at the mesoscale and submesoscale levels. Processes such as mesoscale eddies, submesoscale flows, and internal waves drive intricate energy transfers at these scales. These fine-scale interactions influence the oceanic energy budget through two primary feedback mechanisms: thermal feedback and current feedback. Thermal feedback mainly depletes oceanic potential energy, while current feedback induces a sink of kinetic energy, influencing the kinetic energy pathway. Despite recent advancements, the full impacts of these interactions on the ocean, atmosphere, and climate remain poorly understood. This review synthesizes the current understanding of fine-scale air–sea energetics and their associated effects on the ocean, atmosphere, and climate. It also explores the contributions of submesoscale and high-frequency processes and highlights research gaps. We discuss missing pieces of knowledge, particularly regarding wind-wave effects. Finally, we propose future research directions, emphasizing the need for new observational platforms and next-generation modeling frameworks to capture these interactions and their impact on global climate dynamics.

1. INTRODUCTION

The Earth's oceanic energy cycle is a complex, multiscale system and remains one of the most persistent challenges in physical oceanography and climate science, resulting in significant uncertainties in the climate mean state and its variability. Over the past two decades, significant progress has been made in understanding how energy is exchanged, transformed, and dissipated (or damped) across scales where the ocean and atmosphere interact. At planetary scales [$>\mathcal{O}(100\ \mathrm{km})$], the dynamics are governed primarily by a balance between wind stress curl and Earth's differential rotation (Sverdrup 1947), though this equilibrium is substantially modified by topographic effects and eddy–mean flow interactions, particularly along western boundary regions such as the Gulf Stream (Özgökmen & Chassignet 2002, Schoonover et al. 2016, Debreu et al. 2022).

As illustrated in **Figure 1*a***, the ocean is populated by mesoscale eddies (eddies on horizontal scales of a few hundred kilometers that persist for weeks to months), which account for a large fraction of the ocean's energy reservoir, and submesoscale eddies, fronts, and filaments (0.1–10 km horizontally, 10–100 m vertically, and hours–days temporally), which may be important in the determination of the cross-scale energy transfer. Mesoscale eddies are generated through

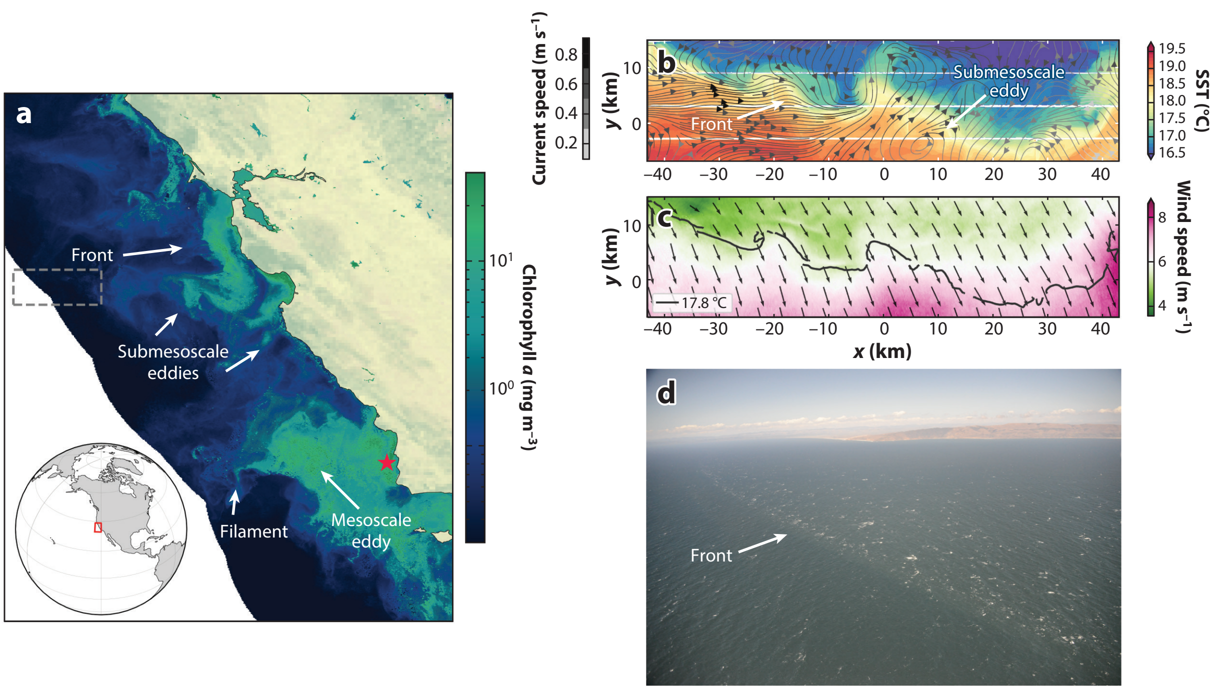

Figure 1

Observational examples of oceanic submesoscale and mesoscale features and air–sea interactions in the California upwelling current system. (*a*) Sea surface chlorophyll *a*, as measured by the Ocean and Land Colour Instrument on Sentinel-3, on September 24, 2019. The dashed gray rectangle shows where the observations in panels *b* and *c* were taken, and the red star shows the approximate location of the image in panel *d*. (*b*) High-resolution airborne measurements of SST (*color scale*) and simultaneously collected surface current streamlines (*gray color scale*) on October 22, 2022. (*c*) Surface wind vectors and speeds on October 22, 2022, with the 17.8° isotherm indicated in black, showing a close correspondence between SST and wind speed anomalies consistent with thermal feedback. (*d*) Photograph of wave modulation across a coastal front near Point Sal, California. Abbreviation: SST, sea surface temperature. Panels *b* and *c* adapted with permission from Farrar et al. (2025); copyright 2025 American Meteorological Society. Panel *d* provided by Nick Statom, Scripps Institution of Oceanography.

baroclinic instability, which converts available potential energy (APE) into kinetic energy (KE), and barotropic instability, which extracts KE from the mean flow (Marchesiello et al. 2003). In addition, mesoscale eddy stirring alters the surface density field, transferring APE to smaller scales via frontogenesis and the formation of submesoscale fronts and instabilities (McWilliams 2016, Klein et al. 2019). These processes further transfer APE into the submesoscale range, where it undergoes baroclinic conversion to KE. At the submesoscale, the effects of rotation and stratification weaken, and vertical velocities associated with unbalanced three-dimensional motions become significant (Taylor & Thompson 2023). Nonlinear advection then affects the turbulent cascade, allowing a transfer of energy toward smaller scales (i.e., a downscale KE flux) (Capet et al. 2008a, Molemaker & McWilliams 2010, Contreras et al. 2023, Srinivasan et al. 2023). The associated mechanisms include frontogenetic secondary circulation, mixed-layer instability, Charney instability (both surface baroclinic instabilities), and a family of ageostrophic instabilities (Capet et al. 2008b, Klein et al. 2008, McWilliams 2016). Submesoscale motions may also contribute to mesoscale reenergization—for example, through the absorption of mixed-layer eddies (Qiu et al. 2014, Schubert et al. 2020, Contreras et al. 2023). Through their vigorous vertical motion and upward heat transport, the submesoscale eddy fields are known to alter the global ocean heat balance, and possibly the mean circulation of the atmosphere (Su et al. 2018).

At higher frequencies, internal waves are generated by various mechanisms, including tidal and wind forcing, as well as spontaneous emission processes arising from loss of geostrophic balance, nonlinear wave–wave interactions, and the formation of lee waves when geostrophic flows interact with seafloor topography (Alford et al. 2016). Many studies have shown that internal waves consistently extract energy from balanced motions, including mean flows, mesoscale eddies, and frontal systems (Bühler & McIntyre 2005, Thomas 2012, Barkan et al. 2015). This energy extraction is subsequently amplified through wave–wave interactions, contributing to the forward cascade of energy (Barkan et al. 2024).

Over the past two decades, the increasing availability of satellite observations and the development of high-resolution coupled ocean–atmosphere models have drawn growing attention to the role of mesoscale and submesoscale ocean–atmosphere interactions in shaping the oceanic energy budget. At fine scales (mesoscale and submesoscale), these interactions act primarily through two feedback mechanisms: thermal feedback (TFB) (Chelton et al. 2004, Xie 2004) and current feedback (CFB) (Renault et al. 2016b, Seo et al. 2016). Both mechanisms influence the oceanic energy budget through two complementary pathways: a KE pathway, associated with the exchange of KE between the ocean KE reservoir and the atmosphere (commonly quantified by the wind work), and a potential energy pathway, associated with the exchange of potential energy between the ocean potential energy reservoir and the atmosphere through diabatic generation or dissipation of potential energy (*GP*) (Bishop et al. 2020).

The wind work can be estimated at different spatial scales. For a given scale σ, it is defined as

$$F_\sigma K_\sigma = \mathbf{u}' \cdot \boldsymbol{\tau}', \qquad 1.$$

where $\mathbf{u}$ denotes the surface current and $\boldsymbol{\tau}$ denotes the surface stress, with primes indicating perturbations at the scale σ. Similarly, the diabatic generation of potential energy, *GP*, can be estimated at different scales. For a given scale σ, its thermal contribution—dominant relative to the freshwater contribution—can be expressed as

$$GP_\sigma = \int_A \frac{\alpha_\theta^2 g}{C_\mathrm{p} N_\mathrm{r}^2} SST' Q'_\mathrm{net} \mathrm{d}A, \qquad 2.$$

where α_θ is the thermal expansion coefficient of seawater, *SST* is the sea surface temperature, Q_net is the net heat flux, g is the gravitational acceleration ($g = 9.81$ m s^{-2}), C_p is the specific heat at constant pressure ($C_p = 4{,}000$ J kg^{-1} °C^{-1}), and N_r^2 is the reference vertical buoyancy gradient (Uchoa et al. 2025), with primes indicating the perturbation at scale σ.

TFB arises from SST anomalies that alter atmospheric stability and surface fluxes, thereby influencing wind patterns and turbulent exchanges (Small et al. 2008, Seo et al. 2023). An example from high-resolution airborne observations is shown in **Figure 1*b*,*c***, where a sharp submesoscale SST front off the California coast leads to strong modulation of the surface wind speeds (Farrar et al. 2025). Energetically, TFB leads predominantly to a depletion of oceanic potential energy at both the mesoscale and submesoscale (through *GP*; **Figure 2**), resulting in a reduction of eddy KE (EKE) (Ma et al. 2016, Bishop et al. 2020, Renault et al. 2023b, Uchoa et al. 2025). As a secondary mechanism, TFB can also induce a transfer of KE between the ocean and the atmosphere (Renault et al. 2024b, 2025) (**Figure 2**). CFB, by contrast, stems from the interaction between ocean surface currents and the atmospheric boundary layer. The relative motion between the ocean and the atmosphere directly modulates the surface stress (Bye 1985). Although wind adjustments partially compensate for these stress changes, the net effect of CFB is a surface stress that opposes the direction of the surface current (Renault et al. 2016a) (**Figure 2**). From an energetic perspective, CFB influences primarily the wind work (i.e., the KE pathway) and to a lesser extent the heat fluxes (Cho et al. 2025), thus also affecting the potential energy pathway. Both pathways operate across ocean mesoscale and submesoscale ranges, yet their net energetic impacts remain poorly constrained and largely absent from most traditional oceanic energy budget and energy cycle frameworks. Additional uncertainty is introduced by surface gravity waves, which have the potential to alter both TFB and CFB by mediating surface momentum fluxes and interacting with boundary-layer turbulence. These effects are also expected to be modulated by mesoscale and submesoscale flows (**Figure 1*d***) but are largely unaccounted for in existing studies of mesoscale and submesoscale air–sea interaction via TFB and CFB.

These studies laid the groundwork for a deeper understanding of mesoscale and, to a lesser extent, submesoscale air–sea interactions, which were later synthesized in comprehensive reviews by Small et al. (2008) and, more recently, by Seo et al. (2023); Gille et al. (2025) provided a synthesis of the fundamental physical processes governing wind–wave–current interactions. Despite these reviews and the recent papers, a critical gap remains: There is currently no comprehensive synthesis that consolidates the energetics of mesoscale and submesoscale air–sea interactions, their direct impact on the ocean energy budget, or the effects of their adjustment on the ocean, atmosphere, and climate. Additionally, the remaining uncertainties and research gaps in this field have not been systematically identified. This review addresses these questions by providing an integrated assessment of the energetics of fine-scale air–sea exchange, accounting for the processes associated with mesoscale and submesoscale eddies, internal waves, and surface gravity waves. We synthesize the current understanding of the energetics of mesoscale and submesoscale air–sea interactions, evaluate the impact of small-scale interactions on larger-scale climate dynamics, and identify gaps in our knowledge, offering insights into future research directions. We also highlight emerging opportunities—from new observational platforms to next-generation coupled modeling frameworks—that are poised to transform our ability to quantify these exchanges.

This article is organized to progressively deepen the exploration of air–sea interaction energetics, starting with established knowledge and moving toward cutting-edge challenges and future directions. We begin in Section 2 by reviewing the state of the art in mesoscale energetics of air–sea interactions, synthesizing current understanding from observational and modeling studies. This section sets the foundation for the discussion by examining how mesoscale processes influence the ocean's energy budget. In Section 3, we delve deeper into submesoscale and high-frequency processes (including inertia gravity waves), which are less understood than mesoscale dynamics but are expected to play a particularly important role in the ocean's forward energy cascade. Here,

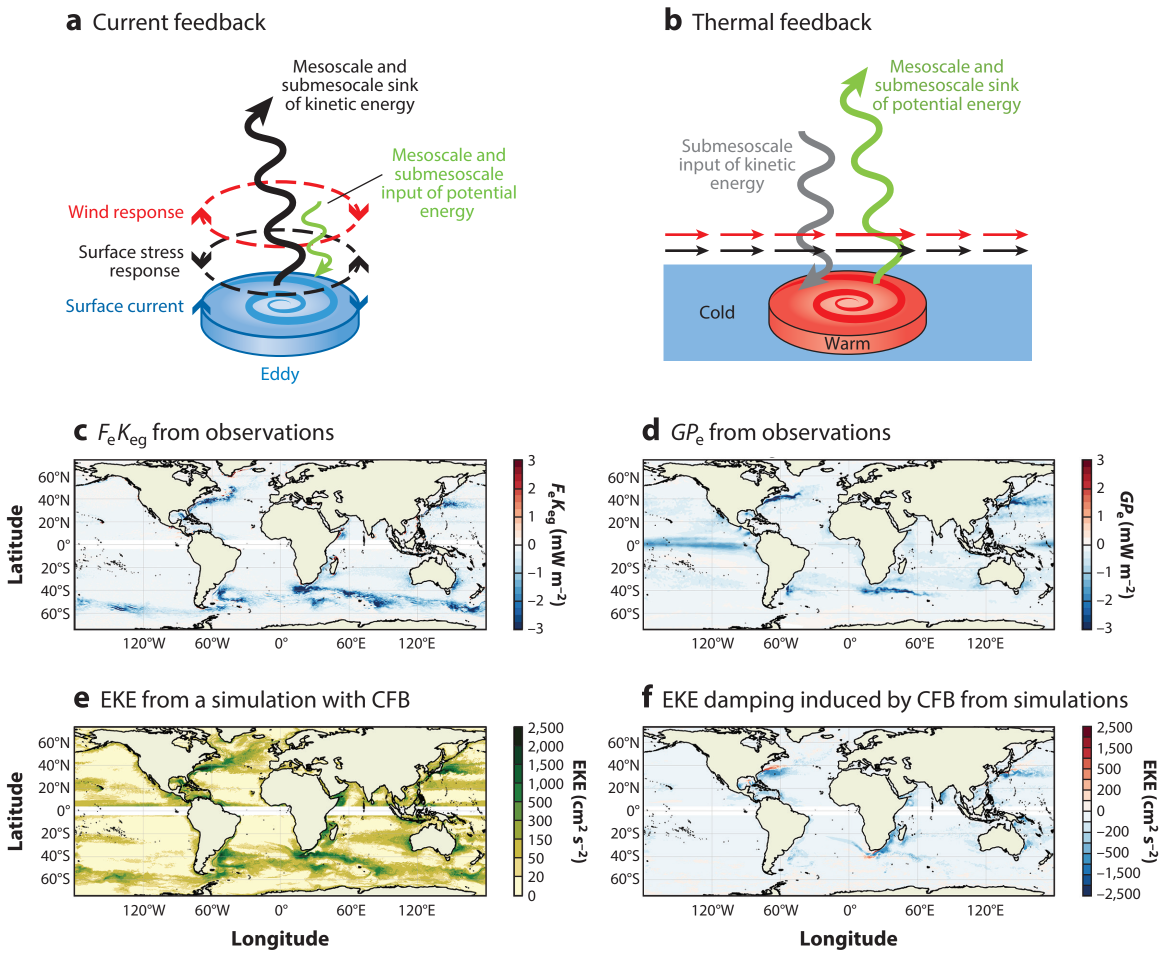

Figure 2

(*a*) Schematic illustrating the main effects of CFB on surface stress, low-level wind, and energy transfer between the ocean and atmosphere. Surface current anomalies (*blue arrows*) induce anticorrelated surface stress anomalies (*black arrows*) and correlated wind anomalies (*red arrows*). Energetically, CFB results in a sink of KE from the ocean to the atmosphere and a weak input of potential energy from the atmosphere to the ocean. (*b*) As in panel *a*, but for TFB. Warm (cold) eddies destabilize (stabilize) the atmospheric boundary layer, accelerating (decelerating) the wind and surface stress. Energetically, TFB induces a submesoscale input of KE (negligible at the mesoscale) and a sink of potential energy at both mesoscale and submesoscale. (*c*) Mesoscale eddy wind work (F_eK_{eg}), estimated from surface stress data from QuikSCAT (Bentamy et al. 2008) and geostrophic current data from AVISO (Ducet et al. 2000) (see Section 2). The sink of KE (negative F_eK_{eg}) is induced primarily by CFB. (*d*) Exchange of potential energy between mesoscale eddies and the atmosphere (GP_e), estimated from observations from J-OFURO and Reynolds et al. (2007) (see Section 2). A negative GP_e indicates a sink of potential energy from the ocean to the atmosphere. GP_e has only a weak impact on mesoscale activity. (*e*) EKE simulated by a global ocean–atmosphere coupled simulation with CFB (Renault et al. 2024a). (*f*) Eddy killing induced by CFB from a global coupled simulation (Renault et al. 2024a), resulting in a damping of the mesoscale activity by approximately 30%. Abbreviations: AVISO, Archiving, Validation, and Interpretation of Satellite Oceanographic Data; CFB, current feedback; EKE, eddy KE; J-OFURO, Japanese Ocean Flux Data Sets with Use of Remote Sensing Observations; KE, kinetic energy; TFB, thermal feedback. Panel *f* adapted with permission from Renault et al. (2024a) (CC BY-NC-ND 4.0).

we explore submesoscale contributions to energy fluxes and the gaps in our current knowledge. Section 4 further investigates the upscaling effects and remote connections of these interactions. Section 5 shifts to emerging perspectives, focusing on the role of surface gravity waves that could modulate both TFB and CFB effects and, thus, the oceanic energy budget. Section 6 reviews observational and modeling challenges in capturing fine-scale air–sea interactions, highlighting the importance of emerging in situ and remote-sensing platforms, advanced models, and improved parameterizations. Key knowledge gaps are identified, and future research directions are proposed to better understand the ocean's energy budget and its complex coupling with the atmosphere and surface waves.

2. MESOSCALE OCEAN–ATMOSPHERE INTERACTIONS

2.1. Current Feedback

At the oceanic mesoscale, CFB mainly acts through the KE pathway via so-called eddy killing (Renault et al. 2016b). This effect systematically extracts KE from mesoscale eddies and transfers it to the atmosphere (**Figure 2**), thereby reducing both the amplitude and vorticity of the eddies (Bye 1985, Renault et al. 2016b, Seo et al. 2016).

In a coupled model or using observations, the surface stress can be estimated using bulk formulas based on the difference between wind and current:

$$\boldsymbol{\tau} = \rho_a C_D (\mathbf{U}_a - \mathbf{U}_o)|\mathbf{U}_a - \mathbf{U}_o|, \quad 3.$$

where $\boldsymbol{\tau}$ is the surface stress, ρ_a is the air density, C_D is the drag coefficient, and $\mathbf{U}_a$ and $\mathbf{U}_o$ are the 10-m wind and surface current, respectively. When neglecting CFB, under the same assumptions, the stress is estimated using only $\mathbf{U}_a$:

$$\boldsymbol{\tau}_a = \rho_a C_D |\mathbf{U}_a| \mathbf{U}_a. \quad 4.$$

The surface stress induced by CFB ($\boldsymbol{\tau}'_{\mathrm{CFB}}$) is therefore the difference between $\boldsymbol{\tau}_a$ and $\boldsymbol{\tau}_r$. As depicted in **Figure 2*a***, a positive current anomaly generates a negative $\boldsymbol{\tau}'_{\mathrm{CFB}}$. Consequently, current anomalies and surface stress anomalies are negatively correlated (Renault et al. 2016b). The KE exchange associated with this process can be estimated as the mesoscale eddy wind work induced by CFB:

$$F_e K_{e\mathrm{CFB}} = \mathbf{u}' \cdot \boldsymbol{\tau}'_{\mathrm{CFB}}, \quad 5.$$

where the primes denote mesoscale anomalies, $\mathbf{u}$ represents surface currents, and $\boldsymbol{\tau}_{\mathrm{CFB}}$ is mesoscale surface stress induced by CFB. $F_e K_{e\mathrm{CFB}}$ reveals a net transfer of KE from the ocean to the atmosphere, as illustrated by the thick black arrow in **Figure 2*a*** (Renault et al. 2016a, 2017b). The atmosphere responds dynamically to this coupling: A negative (positive) surface stress anomaly accelerates (decelerates) the wind (**Figure 2*a***). Thus, the wind anomaly is positively correlated with the surface current. This local acceleration or deceleration of the wind leads to an effect referred to as partial reenergization. It partially compensates for the KE loss, reducing—but not eliminating—the negative wind work. Consequently, the atmospheric response mitigates the efficiency of the eddy-killing effect (Renault et al. 2016b), with the magnitude of this effect varying across spatial scales.

Systematic analyses, integrating satellite observations and numerical simulations, have confirmed that CFB induces a negative eddy wind work across the global ocean (Scott & Xu 2009; Renault et al. 2017a, 2020, 2024a; Jullien et al. 2020; Rai et al. 2021). Although current observations only partially capture the energy exchange, **Figure 2*c*** depicts the KE exchange associated with mesoscale geostrophic eddies, denoted as $F_e K_{eg}$. This field is derived from Archiving, Validation, and Interpretation of Satellite Oceanographic Data (AVISO) geostrophic currents ($\mathbf{u}_g$) (Ducet et al. 2000) and QuikSCAT scatterometer surface stress ($\boldsymbol{\tau}$) (Bentamy et al. 2008) and is expressed as

$$F_eK_{eg} = \mathbf{u}_g' \cdot \boldsymbol{\tau}', \qquad 6.$$

where primes are defined based on spatial or temporal averaging or high-pass filtering (here with a spatial filter with a cutoff of 350 km). The analysis uses nine years of satellite observations. Although F_eK_{eg} does not fully represent F_eK_{eCFB}, it provides an estimate of the local KE exchange rate between mesoscale oceanic currents and the atmosphere. Notably, negative values indicate a transfer of energy from the ocean to the atmosphere. This exchange is most pronounced in regions with strong mesoscale currents and winds, such as western boundary currents and the Southern Ocean. When CFB is neglected, F_eK_{eg} is approximately 0, except in some regions where local dynamics (e.g., orographic winds and island-mass effects) can induce an exchange of KE between the eddies and the atmosphere. At the global scale, these feedback processes contribute significantly to the net transfer of KE from the ocean to the atmosphere, with estimates ranging from 50 to 70 TW (Renault et al. 2017a, Rai et al. 2021), although current observations carry significant uncertainties (Renault et al. 2017a). As discussed in Section 6, simultaneous observations of surface currents and winds are essential for a more accurate characterization of F_eK_{eg}.

EKE is a proxy of the oceanic mesoscale activity and can be estimated as

$$\mathrm{EKE} = 0.5(u_g'^2 + v_g'^2), \qquad 7.$$

As illustrated in **Figure 2*e*,*f***, numerical simulations—with and without CFB—reveal that eddy killing dampens approximately 30% of the EKE (Jullien et al. 2020, Seo et al. 2023). This energy sink significantly exceeds the energy dissipation occurring through the direct KE cascade to submesoscales (Contreras et al. 2023). This damping can be posed as a frictional timescale, which Renault et al. (2016b) estimated at approximately 250 days. Since this timescale is comparable to the lifetime of mesoscale eddies, it further explains the efficiency of CFB in accelerating eddy decay. Without CFB, ocean simulations with rich eddy activity overestimate EKE and key eddy properties, such as lifetime, vorticity, and amplitude. When neglecting CFB, ocean models typically address this bias by introducing artificial diffusion (Chassignet & Xu 2021, Renault et al. 2023a).

The regional variability of the eddy-killing effect arises from the interaction between EKE production and wind intensity, with example estimates of EKE damping of 40% in California (Renault et al. 2016b, Seo et al. 2016), 25% in Peru and Chile, 30% in western boundary currents (Renault et al. 2016a, 2017b; Seo 2017; Larrañaga et al. 2022), 25% in the western Mediterranean Sea and the Pacific equatorial region (Small et al. 2008, Holmes et al. 2024), 24% in the Antarctic Circumpolar Current and Brazil–Malvinas Confluence Zone (Song et al. 2020, Kwak et al. 2021), and nearly 100% in the western Bay of Bengal (Seo et al. 2019).

The damping mainly originates from surface wind work, yet its effects extend throughout the entire depth of the eddies (Renault et al. 2016b, 2023a). CFB can also modify eddy vertical stratification and internal structure. For example, McGillicuddy (2015) showed that eddy–wind interaction induces Ekman pumping, whose sign depends on eddy vorticity, altering the upper pycnocline structure by producing mode water–like cores in anticyclones and thinner, surface-intensified cyclonic structures. This mechanistic result indicates that, while CFB contributes to net EKE damping, it can also systematically reshape eddy vertical structure, highlighting the need to examine the vertical distribution of CFB effects in future studies, particularly given their implications for nutrient supply, biogeochemical cycling, and biological productivity (McGillicuddy et al. 2007).

CFB also affects key energy conversions—such as barotropic and baroclinic processes (e.g., Marchesiello et al. 2003)—by modulating the large-scale circulation (see also Section 4 for upscaling impacts). For instance, CFB has been shown to slow down mean gyres (Luo et al. 2005), thereby reducing barotropic conversion, as observed in the Pacific equatorial region (Holmes et al. 2024). Meanwhile, local changes in stratification or vertical shear can alter baroclinic energy transfer, particularly in systems like the Agulhas Current (Renault et al. 2017b). Additionally, CFB influences turbulent heat fluxes (e.g., Cho et al. 2025), potentially creating an energy pathway that modifies mesoscale APE and its baroclinic conversion to KE. This mechanism may be especially relevant in regions with weak winds and strong currents, such as the equatorial zone. However, while these effects warrant further investigation, they appear to be secondary compared with the dominant energetic signature of CFB: the damping of mesoscale activity through eddy killing.

2.2. Thermal Feedback

TFB is a distinct coupling mechanism driven by SST anomalies that modify turbulent heat fluxes, the marine atmospheric boundary layer, the associated near-surface wind, and, thus, the surface stress. Energetically, TFB can act through both the kinetic and the potential pathways of energy (Ma et al. 2016, Seo et al. 2016, Bishop et al. 2020, Renault et al. 2023a). The KE exchange associated with TFB can be estimated as the mesoscale eddy wind work induced by TFB:

$$F_e K_{eTFB} = \mathbf{u}' \cdot \boldsymbol{\tau}'_{TFB}, \qquad 8.$$

where the primes denote mesoscale anomalies, and $\boldsymbol{\tau}_{TFB}$ is the mesoscale surface stress induced by TFB. However, because mesoscale TFB-induced wind anomalies are generally incoherent with the underlying oceanic currents, $F_e K_{eTFB}$ remains negligible (Renault et al. 2017b, 2019b), and TFB does not directly remove KE from the mesoscale eddies (Seo et al. 2016, Renault et al. 2023b). Since TFB can alter the potential-to-kinetic energy pathway by weakening baroclinic instability near the surface, TFB acts primarily as a sink of potential energy (hereafter denoted GP_e; **Figure 2*b***) as SST-induced buoyancy fluxes extract potential energy from the oceanic mixed layer (Bishop et al. 2020). Note that CFB can also modulate turbulent heat fluxes (Cho et al. 2025), leading to a secondary contribution to GP_e (Seo et al. 2021).

To quantify GP_e, we follow Bishop et al. (2020) and Equation 2 and estimate the thermal contribution to TFB at the mesoscale—defined here as deviations from a monthly climatology—using monthly net heat fluxes (Q_{net}) from Japanese Ocean Flux Data Sets with Use of Remote Sensing Observations Version 3 (J-OFURO3) (Tomita et al. 2019) and daily SST data from Reynolds et al. (2007) over the period 1988–2017. We also use the Monthly Isopycnal and Mixed-Layer Ocean Climatology (MIMOC) (Schmidtko et al. 2013) to derive the thermal expansion coefficient (α_θ) and the background reference buoyancy frequency ($N_r = 5.2 \times 10^{-3}$ s^{-1}, following Bishop et al. 2020). As illustrated in **Figure 2*d***, consistent with previous studies (Bishop et al. 2020), GP_e is predominantly negative, indicating a net sink of potential energy from mesoscale eddies to the atmosphere. The strongest potential energy sinks occur over western boundary currents (e.g., Bishop et al. 2020, Seo et al. 2021). Consistent with the study by Bishop et al. (2020), the surface area integrated GP_e is negative, with a value of −0.087 TW. This loss of potential energy reduces the baroclinic conversion of APE into EKE, thereby dampening the growth of mesoscale instabilities (Ma et al. 2016, Renault et al. 2023b). The influence of TFB through GP_e is confined to the upper tens of meters, where turbulent heat fluxes dominate. Its impact diminishes with depth and exhibits marked spatial variability (Renault et al. 2023b). TFB is most effective in regions characterized by strong SST gradients, such as western boundary currents and the equatorial region (Ma et al. 2016, Renault et al. 2023b, Holmes et al. 2024).

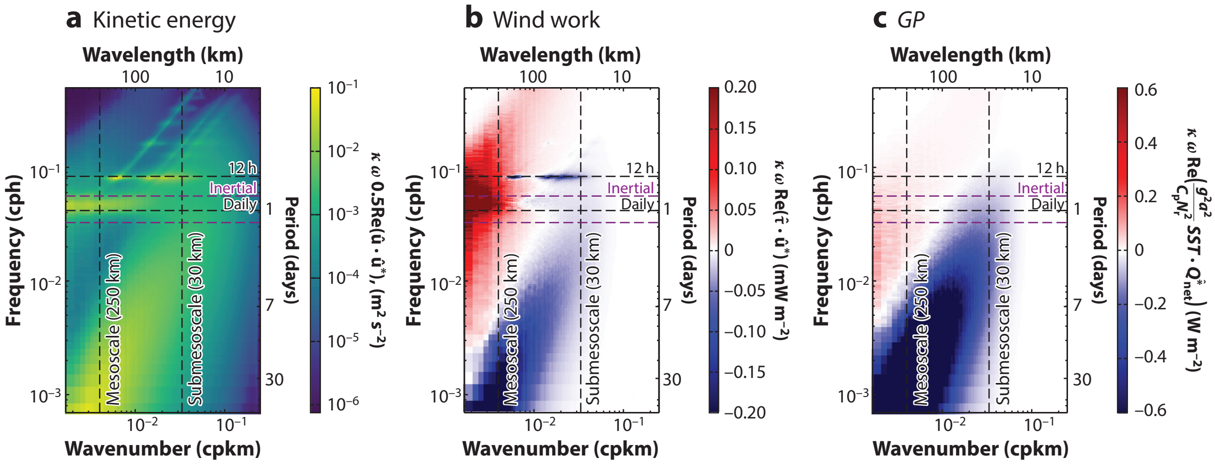

Figure 3

Frequency–wavenumber cospectra of (*a*) kinetic energy, (*b*) wind work, and (*c*) potential energy transfer (*GP*). Each cospectrum is multiplied by the wavenumber (k) and frequency (ω) in order to highlight the variance in the spectral space. The cospectra are estimated over a five-year period in the Gulf Stream region using a coupled submesoscale ocean–atmosphere–wave simulation with a spatial resolution of $dx = 2$ km (Contreras et al. 2023, Larrañaga et al. 2025). The dashed purple lines indicate the limits of the near-inertial frequency band for the range of latitudes simulated. Abbreviations: cph, cycles per hour; cpkm, cycles per kilometer.

3. HIGH-FREQUENCY OCEAN–ATMOSPHERE INTERACTIONS

The results of the preceding section focused on the ocean mesoscale, characterized by spatial scales of order 10–100 km, with timescales of order days to weeks. However, significant near-surface variability exists at smaller horizontal scales of order 1–10 km, evolving at timescales between hours and days. This is illustrated in **Figure 3**, which shows the wavenumber–frequency cospectra of KE (**Figure 3*a***), wind work (as cospectra of surface current and surface stress) (**Figure 3*b***), and potential energy transfer (*GP* as cospectra of SST and net heat flux) (**Figure 3*c***) in the Gulf Stream, fully derived from an ocean–atmosphere–wave coupled simulation with 2-km horizontal resolution (Contreras et al. 2023, Larrañaga et al. 2025) for a period of five years. Consistent with previous studies (e.g., Torres et al. 2022a, Delpech et al. 2023), the dominant reservoir of energy is found at mesoscale wavelengths. In terms of KE, these spatiotemporal scales can be further partitioned into quasi-balanced motions associated with submesoscale fronts and eddies—whose energy is concentrated primarily at slightly subinertial frequencies and follows an approximately linear increase of frequency with wavenumber (Torres et al. 2022a, Tedesco et al. 2024)—and unbalanced internal gravity waves (IGWs), which populate higher frequencies, particularly near the inertial band and along the dispersion curves of baroclinic tides (Delpech et al. 2023, Tedesco et al. 2024). Both the submesoscale and IGWs are understood to play central roles in ocean energetics through the generation of downscale energy transfers to turbulence and, for the submesoscale, seasonally varying upscale and downscale energy transfers with the mesoscale (Garabato et al. 2022).

As shown in **Figure 3**, the essential mechanisms of air–sea interaction discussed above, the TFB and CFB, are also active for these higher-frequency motions; however, the dynamical response and energetic consequences may differ. The submesoscale is characterized dynamically in part by Rossby numbers of order unity, and it occupies spatial scales that overlap with the atmospheric microscale and meso-γ scales, such that the dynamics of both fluids are nonlinear (Nuijens et al. 2024). Likewise, the fast timescales of the submesoscale and IGWs challenge conceptual models of air–sea coupling that assume a steady-state response. Air–sea interactions at this scale are therefore expected to be characterized by significant imbalances between ocean and atmosphere, strong advective contributions (possibly in both mean and turbulent scale properties), and potentially distinct pathways to modifying the energetics. In this section, we review what is known about high-frequency air–sea interactions and highlight open questions and challenges.

3.1. Feedbacks on Submesoscales

The CFB-induced wind stress anomaly originates primarily from consideration of the surface-relative wind speed as opposed to the Earth-relative wind speed. As such, this portion of the CFB is expected to be active regardless of the spatial or temporal scale. This is confirmed by **Figure 3*c***, which reveals the presence of a sink of KE at the submesoscale. In contrast, however, the atmospheric dynamical response to CFB-induced wind stress anomalies, which modifies surface winds in a manner that partially compensates for the surface current effects (**Figure 2*a***), is scale dependent. Coupled numerical models indicate a weaker compensating wind response at the submesoscale compared with the mesoscale such that the submesoscale CFB is approximately 30% more effective than the mesoscale (Renault et al. 2024b, 2025; Conejero et al. 2024). However, as demonstrated by Renault et al. (2024b), the short lifetime of submesoscale eddies, compared with the frictional timescale associated with CFB (17.5 days for submesoscales), limits the impact of the eddy-killing process on submesoscale activity. This results in a relatively modest reduction in surface KE, on the order of 10% for the Gulf Stream (Renault et al. 2024b).

In addition to wind work, CFB may affect submesoscale energetics through its effect on buoyancy fluxes. Notably, strong wind stress curls introduced by CFB at the submesoscale modify the Ekman contribution to the vertical buoyancy flux. Coupled numerical experiments investigating the California Current System and Gulf Stream indicate that submesoscale CFB enhances baroclinic conversion of potential energy to KE by $\mathcal{O}(10\%)$ (Renault et al. 2018, 2024b). At the same time, CFB also leads to a systematic reduction of the component of the wind stress aligned with the surface thermal wind shear (the downfront wind), which acts to reduce the horizontal cross-frontal Ekman buoyancy flux (Wenegrat 2023). This advective buoyancy flux, along with the associated surface potential vorticity flux, is negligible at large scales but is known to exert a strong control on boundary-layer processes at the submesoscale (Taylor & Ferrari 2010, D'Asaro et al. 2011). Importantly, winds aligned with fronts introduce a bidirectional energy exchange between fronts and turbulence (upscale for upfront winds, downscale for downfront winds) (Zheng et al. 2025), which recent global estimates suggest may play a major role in energizing boundary-layer turbulence and enhancing dissipation of KE (Dong et al. 2024). The extent to which air–sea coupling and CFB modify these estimates remains to be quantified.

Both observations and models also indicate strong modulation of air–sea heat fluxes at submesoscale fronts (Iyer et al. 2022a, Renault et al. 2024b, Shao & Wu 2024). Even though the horizontal scale of submesoscale fronts is close to the typical vertical scales of the planetary boundary layer (such that the aspect ratio is not small), large eddy simulation indicates that submesoscale surface heat fluxes can force a rapid dynamical adjustment of the marine atmospheric boundary layer—involving the development of shallow internal boundary layers through both vertical mixing and horizontal advection—such that there is a strong response of surface winds to submesoscale SST fronts (Skyllingstad et al. 2007, Wenegrat & Arthur 2018, Sullivan et al. 2020, Kaouah et al. 2025). Recent high-resolution process-study observations have confirmed these model predictions, emphasizing that the small spatial scales of the response are associated with the generation of large [$\mathcal{O}(f)$] horizontal divergence or curl in the surface wind stress (depending on the wind front alignment) (Wineteer et al. 2024, Farrar et al. 2025). However, despite these strong responses, the direct energetic effects on the submesoscale appear to be limited. Unlike at the mesoscale, the interplay between submesoscale TFB and CFB modulates both surface stress and wind. Specifically, TFB-induced stress and wind anomalies exhibit spatial coherence with surface currents, resulting in either constructive or destructive effects on surface stress and submesoscale wind work. These effects depend on the local characteristics of SST gradients and vorticity (Bai et al. 2023, Conejero et al. 2024). While generally modest, this interaction can weakly energize submesoscale currents, contributing less than 5% to their KE budget (Renault et al. 2024b, 2025). Second, while the strong wind stress curls have been interpreted in terms of the implied large Ekman pumping velocities and associated vertical buoyancy fluxes, the fast timescales of these processes call into question the validity of the steady-state Ekman assumptions.

Instead, as at the mesoscale, the energetic impact of the TFB response at the submesoscale appears to be dominated by the direct flux of APE associated with the correlation of surface buoyancy and buoyancy flux anomalies (Uchoa et al. 2025). Coupled numerical experiments over both the Gulf Stream and California Current System show that submesoscale surface APE flux leads to a significant (10–50%) reduction of submesoscale APE, a stronger effect than eddy killing at small scales (Renault et al. 2024b, Uchoa et al. 2025). This flux of potential energy can also be seen in **Figure 3*c***. This reduction of APE in turn reduces vertical buoyancy production and consequently appears as a reduction in submesoscale KE. Finally, we note that uncoupled global submesoscale-permitting numerical models suggest a large rectified contribution of approximately 20 W m^{-2} of additional air–sea heat fluxes from high-frequency submesoscale motions (Su et al. 2018). This would be a significant missing source of air–sea exchange in lower-resolution models; however, the quantitative uncertainty introduced by the use of an uncoupled ocean model is currently unclear. The next generation of high-resolution coupled global modeling efforts currently underway will allow for this question to be addressed.

3.2. Feedbacks on Internal Gravity Waves

Coupled air–sea interactions also have strong effects on the energetics of IGWs. Previous work has focused on near-inertial (NI) waves, showing the damping effect of CFB on NI energy. Rath et al. (2013) found that including CFB in the surface stress formulation reduced NI energy by 40% in a mesoscale-permitting forced model of the Southern Ocean. This was attributed to a reduction of NI wind work of approximately 20%. Similar-magnitude reductions of NI wind work were found under the storm tracks of the subtropical North Pacific and Atlantic using reanalysis winds with a slab ocean model (Zhai 2017), although the precise value may be sensitive to how NI energy is dissipated or transferred through the base of the mixed layer (Alford 2020). A global evaluation using surface drifters likewise found that not including surface currents in the calculation of wind stress could lead to local errors in NI wind power input as large as 120% of the total, with a global average error of 60% (Liu et al. 2019). Importantly, however, these prior estimates have not accounted for the potential increase in surface winds associated with CFB, which could offset a portion of the estimated reduction, although the high-frequency response of surface winds to CFB is not currently known (see Conejero et al. 2024 and Section 6).

The strength and sign of the CFB effect vary across wavenumber–frequency space. In the NI band, models indicate positive wind work for scales larger than approximately 200 km and negative wind work (internal wave killing) at smaller scales (Flexas et al. 2019, Torres et al. 2022b, Delpech et al. 2023). This can be seen for a simulation of the subtropical North Atlantic in **Figure 3*b***. Similar damping of mixed-layer KE is also evident along the dispersion curves for baroclinic tides, with an effect that was quantified in the California Current System to represent approximately 10% of the total barotropic to baroclinic tidal conversion (Delpech et al. 2023). In regions where the ocean tidal velocities can become large, such as shallow shelf seas, this effect becomes strong enough to lead to an appreciable increase in variance in the surface winds at the tidal frequency (Renault & Marchesiello 2022).

Less is known about the effect of TFB on IGWs. Pure NI waves do not carry potential energy, and for superinertial waves, the kinetic to potential energy ratio is much larger than unity outside of the tropics (Buijsman et al. 2025). The flux of APE due to TFB is thus expected to not significantly affect wave energetics, in contrast to the effect on balanced motions, as discussed above (supported by calculations of *GP* in wavenumber–frequency space; **Figure 3**). Whether the TFB modification of surface winds contributes to the energetics of IGWs is also not currently known. To the extent that results considering low-frequency motions are applicable to understanding IGWs, it can be anticipated that the small-spatial-scale wind anomalies introduced by TFB may contribute to the generation of high-wavenumber variability in the NI wavefield and consequently to inertial pumping. However, assessing these interactions and their effects on energetics requires the use of high-resolution coupled models so as to accurately account for the joint evolution of atmospheric and oceanic boundary-layer processes.

Finally, air–sea coupling may influence interactions between balanced flows and IGWs, which modulate energy cascades by weakening the mesoscale inverse cascade and enhancing the submesoscale forward cascade (Thomas & Daniel 2021, Barkan et al. 2024, Tedesco et al. 2024). Both TFB and CFB affect energetics in a scale-dependent manner, complicating predictions of their net impact on balanced-wave interactions. Nevertheless, coupled models that resolve the full flow likely already capture these effects, though their significance remains to be quantified and incorporated into conceptual frameworks.

4. UPSCALING AND REMOTE CONNECTIONS

In the ocean, mesoscale eddies interact with the large-scale circulation through eddy–mean flow interaction, driving an inverse KE cascade (e.g., Capet et al. 2008a, LaCasce 2012). Given that mesoscale eddies represent a dominant reservoir of oceanic KE, this inverse cascade plays a critical role in regulating the general circulation. As discussed below, a reduction of oceanic mesoscale activity—by approximately 30% on average through eddy killing—weakens the turbulent cascade, which has significant implications for ocean dynamics.

Following Marchesiello et al. (2011), the spectral KE flux $\Pi(k)$, representing the rate of energy transfer across wavenumbers, is obtained by integrating in k the KE advection term $A(k)$, assuming that the flux vanishes at the highest wavenumber k_{max}. The expression for $A(k)$ is

$$A(k) = A_{\mathrm{H}}(k) + A_{\mathrm{V}}(k) = \Re\left[\overline{-\widehat{\mathbf{u}}_{\mathrm{h}}^{*} \cdot \widehat{(\mathbf{u}_{\mathrm{h}} \cdot \nabla)\mathbf{u}_{\mathrm{h}}} - \widehat{\mathbf{u}}_{\mathrm{h}}^{*} \cdot \widehat{w\frac{\partial \mathbf{u}_{\mathrm{h}}}{\partial z}}}\right]. \qquad 9.$$

Here, the hats denote a horizontal Fourier transform applied after removing the areal mean and applying either windowing or symmetrization to minimize edge effects during periodization. The asterisks denote the complex conjugate, $\mathbf{u}_{\mathrm{h}}$ represents the horizontal ocean currents, w is the vertical velocity, $\Re$ indicates the real part, and the overbar represents a temporal average over the full simulation period (multiple years). The KE flux $\Pi(k)$ is then computed as

$$\Pi(k) = \int_{k}^{k_{\mathrm{max}}} A\,\mathrm{d}k. \qquad 10.$$

Using this formulation, Renault et al. (2019a) estimated the energy flux Π for the Gulf Stream and the Agulhas Current based on surface geostrophic currents—the primary drivers of the inverse energy cascade (Contreras et al. 2023). As shown in **Figure 4*a***, simulations incorporating

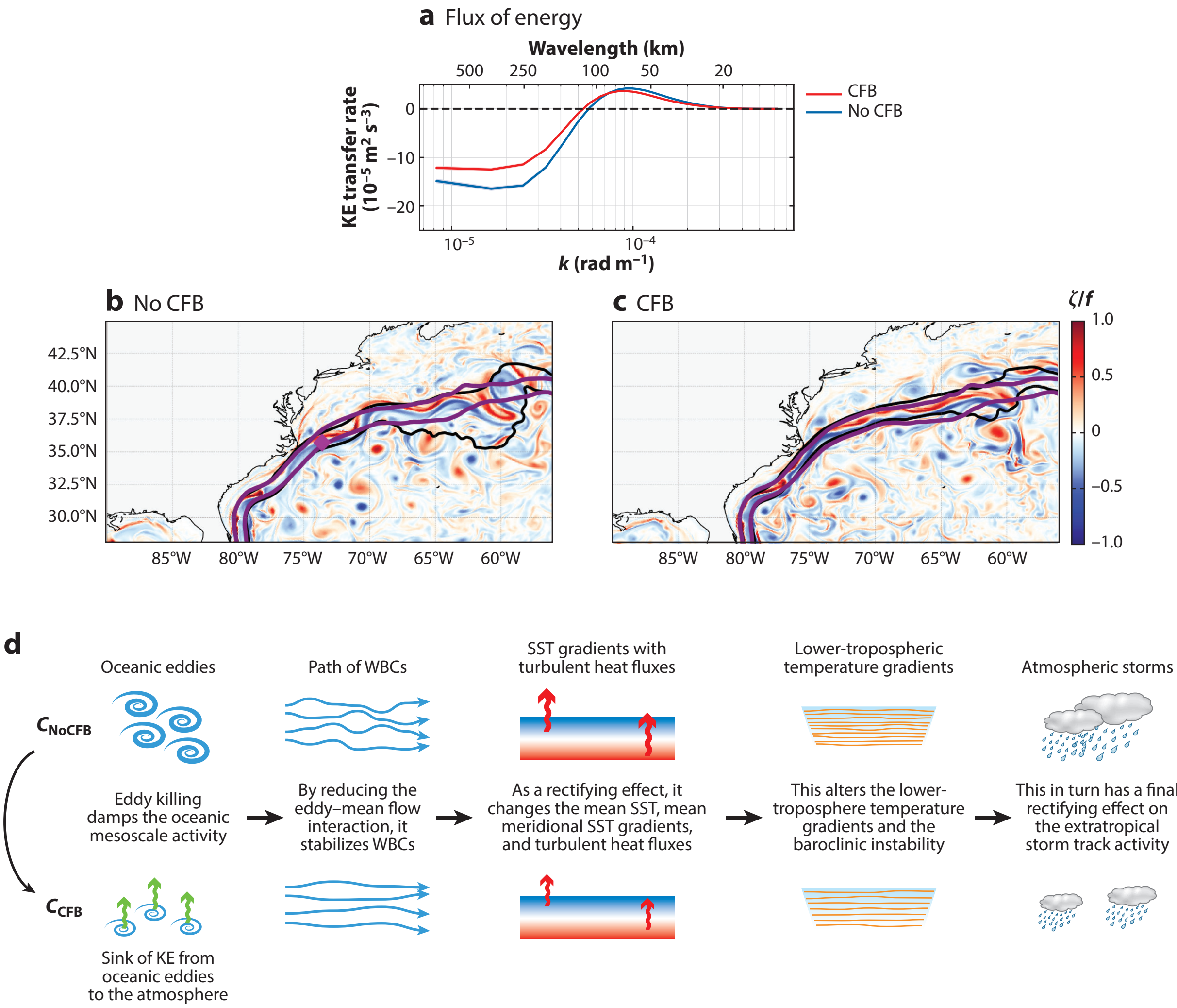

Figure 4

(*a*) Cascade of geostrophic kinetic energy over the Gulf Stream from an ocean–atmosphere mesoscale-resolving simulation without (*blue*) and with (*red*) CFB (for details, see Renault et al. 2019a). (*b*,*c*) Snapshots of surface relative vorticity from coupled simulations without (panel *b*) and with (panel *c*) CFB. Black contours indicate the simulated long-term mean Gulf Stream path (0.6 m s^{-1}); purple contours show the observed Gulf Stream path (0.6 m s^{-1}). (*d*) Schematic illustration of the sequence of processes induced by mesoscale CFB. Abbreviations: CFB, current feedback; KE, kinetic energy; SST, sea surface temperature; WBC, western boundary current. Figure adapted with permission from Renault et al. (2024a) (CC BY-NC-ND 4.0).

CFB (i.e., eddy killing) weaken the inverse cascade compared with those without CFB. This stabilization effectively reduces long-standing model biases in representing major current systems. For instance, the Gulf Stream becomes excessively meandering in simulations without CFB, as eddy–mean flow interactions are overestimated (**Figure 4*b***) (Renault et al. 2016a, 2019a). Similar stabilizing effects have been documented for other regions (Renault et al. 2017b, Seo 2017, Larrañaga et al. 2022).

The stabilization of boundary currents and fronts has notable consequences for large-scale SST patterns and their horizontal gradients (Renault et al. 2024a). In regions such as the Agulhas

Current, the damping of mesoscale activity reduces advection of warm waters from the Indian Ocean into the South Atlantic. This modifies the cross-basin temperature gradient and alters the heat transport associated with Agulhas leakage (Renault et al. 2017b, Seo et al. 2021). Similar behavior can be observed for the Gulf Stream (Renault et al. 2024a). These SST adjustments influence the atmosphere by altering both the surface turbulent fluxes and the lower-tropospheric temperature gradients. Changes in SST gradients also modify air–sea heat and moisture exchanges. They alter the lower-tropospheric temperature gradients and, consequently, the atmospheric baroclinicity. This modulation of baroclinic energy conversion in the lower atmosphere affects the intensity of extratropical storms (by up to 15% in western boundary current regions) (Seo et al. 2021, Renault et al. 2024a). The impact on storm frequency is still unknown. These results suggest that modulating the ocean's energy budget through mesoscale coupling contributes to large-scale climate variability by influencing oceanic fronts, surface fluxes, and ultimately the atmospheric energy cycle.

The potential tropical consequences remain largely unexplored. In the equatorial Pacific, changes in SST patterns driven by eddy killing (Renault et al. 2024a) and current stabilization could influence the Walker and Hadley circulations. This could potentially modify the asymmetry and frequency of El Niño–Southern Oscillation events. Future research should evaluate the impact of mesoscale air–sea coupling on the Intertropical Convergence Zone and other large-scale climate patterns.

5. SURFACE WIND WAVES: A MISSING PIECE OF THE PUZZLE?

Sections 2–4 explored fine-scale air–sea energetics, focusing on two key feedback mechanisms: CFB, which operates primarily through the KE pathway via wind work and eddy killing, and TFB, which influences the potential energy pathway through diabatic potential energy fluxes. Surface gravity waves introduce an additional layer of complexity that is not readily captured by either feedback process. Sea state responds to local wind forcing, carries nonlocal memory in the form of swell, and is strongly modified by ocean currents and density fronts (**Figure 1*d***). As a result, waves can modulate (*a*) the magnitude and direction of the surface stress that enters the wind work, which are central to CFB, and (*b*) near-surface ocean turbulence and dissipation, which can indirectly influence TFB through relevant quantities such as SST, mixed-layer depth, and heat fluxes.

Wave–wind and wave–current interactions are active research areas in their own right (e.g., Gille et al. 2025). However, from the energetic perspective adopted here, their importance lies in the strong spatial heterogeneity introduced in surface drag and upper-ocean mixing at scales comparable to ocean mesoscale and submesoscale variability. This raises two questions: To what extent does sea state–driven variability in momentum flux and near-surface dissipation alter the diagnosed energetics of CFB and TFB, and can such effects systematically rectify onto larger scales, such as boundary currents and storm tracks? In the following, we summarize the relevant mechanisms with an emphasis on their parameterization, energetic signatures, and remaining uncertainties.

5.1. Wave–Wind Interaction

Wave–wind coupling supports the exchange of momentum, heat, and moisture across the atmospheric and oceanic boundary layers, with wind-forced short waves playing a dominant role in setting surface roughness and momentum exchange process (e.g., Edson et al. 2013, Sullivan et al. 2018). Bulk flux algorithms represent wave effects on wind stress through a wave roughness length (z_0) parameterization that depends primarily on wind speed. This formulation does retain implicit consideration of sea state as it is based on the observed quasi-linear relationship between natural wind speed and inverse wave age, commonly defined by ratios such as c_p/U_{10} or c_p/u_*, for winds in the 5–15 m s^{-1} range. This formulation is consistent with the equilibrium sea state concept of Phillips (1985), in which wind input to the wave field is locally balanced by dissipation through wave breaking and nonlinear wave–wave interactions (Csanady & Gibson 2001). Observational studies have provided support for this equilibrium framework, including details on turbulent dissipation rates immediately below the surface (e.g., Thomson et al. 2013). As a result, parameterizations based on a wind speed–dependent Charnock parameter (α) and z_0 skillfully reproduce time-averaged statistics of observed air–sea fluxes over much of the open ocean and are therefore widely adopted in studies diagnosing CFB energetics.

Wave–wind equilibrium assumptions often break down in dynamically active regions that dominate fine-scale air–sea interactions. Rapidly moving storms, limited coastal fetch, strong surface vorticity and density gradients, and the coexistence of swell and wind waves generate mixed, nonequilibrium sea states in which dominant waves may be poorly correlated with local winds or currents. In such environments, common in western boundary currents, air–sea momentum exchange depends not only on instantaneous wind forcing but also on the evolving sea state. These departures from equilibrium have direct implications for the KE pathway. Because wind work depends on stress–current correlations, sea state–dependent modifications of surface stress can alter diagnosed energy transfers. Wave effects may amplify or damp the eddy-killing effect, introduce additional stress–current covariance beyond CFB, and modify the partitioning of wind work across mesoscale and submesoscale frequencies. In this way, waves can reshape both the magnitude and spatial structure of CFB.

Sea state–dependent stress parameterizations provide one pathway to represent these effects. One class relates z_0 explicitly (rather than implicitly) to wave age, while complementary approaches incorporate significant wave height (H_s) as a proxy for wave steepness and breaking propensity (Donelan 1990, Edson et al. 2013). These formulations are particularly relevant in environments influenced by strong current gradients or rapidly evolving winds, where refraction, Doppler shifting, and the coexistence of wind sea and swell decouple sea state from local atmospheric forcing (Iyer et al. 2022b; Sauvage et al. 2023, 2024). Approaches exist that incorporate the directional wave–wind coupling, recognizing that the directional misalignment produces anisotropic surface roughness (Chen et al. 2013, Porchetta et al. 2021, Sauvage et al. 2023). Such formulations can substantially modify z_0 and C_D under specific wave–wind misaligned conditions (Patton et al. 2019, Husain et al. 2022) and can improve agreement with direct covariance flux measurements in some settings (Sauvage et al. 2024, Raj et al. 2025). The extent to which these formulations modify inferred CFB energetics in western boundary current regions and other regions of strong mesoscale air–sea interaction remains to be systematically evaluated.

An illustration of the energetic implications of wave–wind misalignment is provided in **Figure 5*a*–*f***, which combines a coupled model simulation and moored direct covariance flux and wave observations during the passage of an atmospheric cold front off the US East Coast. The abrupt rotation of surface winds associated with frontal passage, together with the finite adjustment time of the wave field, generates an extensive region behind the cold front in which dominant southerly surface waves propagate in a direction different from that of postfrontal northwesterly winds. As shown in **Figure 5*e***, this misalignment is captured consistently in both observations and the coupled model.

Such conditions violate the equilibrium assumptions underlying wind speed–only z_0 parameterizations and lead to anisotropic surface roughness that serves as an additional roughness element. When wave–wind misalignment is accounted for in the Coupled Ocean–Atmosphere Response Experiment (COARE) bulk flux formulation (Sauvage et al. 2023), over a timescale of 6 h, the effective roughness length z_0 increases by approximately 100–300%, the drag coefficient

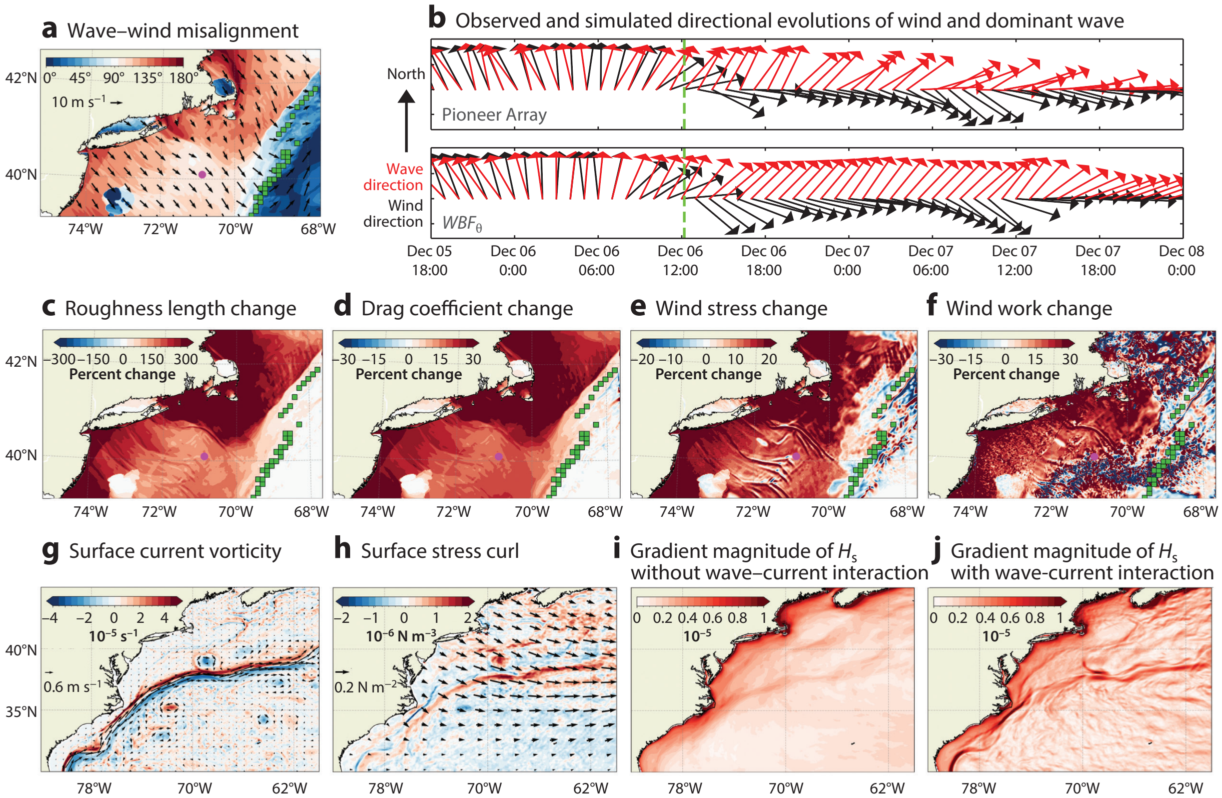

Figure 5

(*a–f*) Impacts of wave–wind interaction behind an atmospheric cold front at 15:00 UTC on December 6, 2016. (*a*) Absolute angle (θ) between wind and dominant wave directions simulated with a coupled model that included wave–wind directional coupling (WBF_θ); the green markers indicate the detected cold front, the black arrows denote wind direction, and the magenta circle marks the location of the Ocean Observatories Initiative Pioneer Array. (*b*) Hourly time series of wind (*black*) and dominant wave (*red*) directions from Pioneer Array observations and the coupled model (WBF_θ); the green dashed line denotes the time of frontal passage at the array. (*c–f*) Changes in roughness length (z_0) (panel *c*), drag coefficient (C_D) (panel *d*), wind stress ($\boldsymbol{\tau}$) (panel *e*), and wind work (panel *f*) associated with wave–wind misalignment, diagnosed from coupled model simulations with and without directional wave–wind coupling in the surface roughness parameterization. (*g–j*) Climatological effects of wave–current interaction from coupled model simulations over the Gulf Stream: surface current vorticity (panel *g*), surface wind stress curl (panel *h*), and magnitudes of the horizontal gradient of significant wave height ($|\nabla H_s|$) with and without wave–current interaction enabled (panels *i* and *j*, respectively). Panels *a–f* adapted from Sauvage et al. (2024).

C_D increases by 10–30%, and the estimated momentum flux $\boldsymbol{\tau}$ increases by 10–20%. The enhanced stress translates into a 15–30% increase in wind work. As demonstrated by Sauvage et al. (2024), taking this effect into consideration brings the surface stress estimates closer to the direct covariance flux from the Pioneer Array.

From the energetics perspective discussed here, this example highlights how transient, nonequilibrium sea states can alter wind work diagnostics central to CFB. Hence, this process may represent a mechanism by which wave dynamics can amplify or weaken diagnosed eddy killing, particularly in frontal and storm track regions, where such misalignment events are frequent. However, the long-term climatological impact of wave-mediated modifications to wind work estimates remains largely unexplored, with only a limited number of studies addressing this issue to date (e.g., Zhang et al. 2021). Quantifying these effects requires coordinated observations and coupled modeling of winds, directional waves, upper-ocean currents, and direct covariance and bulk fluxes at consistent scales—capabilities that are increasingly accessible through emerging observational platforms and fully coupled modeling frameworks (Section 6).

5.2. Wave–Current Interaction

Surface currents strongly influence wave evolution through refraction, Doppler shifting, and convergence or divergence of wave action across vorticity and strain features, modulating wave height and, more generally, the shape of the wave spectrum and the associated wave parameters, such as wavelength, mean square slope, and directional spreading (Phillips 1966, Bretherton & Garrett 1968, Ortiz-Suslow et al. 2025). Opposing currents steepen waves and increase breaking probability, while following currents flatten waves and suppress breaking (Chawla & Kirby 2002, VreĆica et al. 2022). Refraction across rotational currents can produce spatially variable wave directions that differ from the local wind direction (Villas Bôas et al. 2020, Marechal & de Marez 2022, Wang et al. 2023). As a result, surface currents lead to spatially coherent heterogeneity in sea state and, consequently, in surface drag with the ocean currents (Ardhuin et al. 2017, Villas Bôas et al. 2025).

Mesoscale and submesoscale currents can imprint on air–sea momentum fluxes by modulating the sea state and thus surface drag (Edson et al. 2013). Under opposing wave–current conditions, wave steepness increases, enhancing breaking and roughness, which may intensify the extraction of ocean KE through wind work. Conversely, aligned wave–current configurations reduce effective roughness and may alter momentum transfer efficiency. Because these wave effects covary with fronts and eddies that govern TFB and CFB, wave–current interactions may be dynamically correlated with fine-scale kinetic and potential energy pathways. Recent kilometer-scale Surface Water and Ocean Topography (SWOT) Ka-Band Radar Interferometer observations have provided event-scale evidence of this coupling. Villas Bôas et al. (2025) reported sharp spatial gradients in H_s across the Gulf Stream and other energetic regions, consistent with theoretical expectations of wave refraction (Wang et al. 2025), focusing, and steepening by strong currents. Complementary coupled simulations (**Figure 5*g–j***) show that when wave–current interaction is activated, surface wave energy is redistributed by the vorticity field, producing coherent H_s gradients aligned with mesoscale structures; when the interaction is disabled, this spatial coherence vanishes. Hence, the satellite remote sensing and numerical models demonstrate that wave–current interaction provides a robust physical pathway through which fine-scale currents shape sea state heterogeneity and modulate air–sea momentum exchange, with direct implications for surface drag and wind work diagnostics.

Wave–current interaction also affects the turbulence KE budget of the upper ocean. Wave breaking injects turbulence KE and enhances dissipation within a near-surface layer of order H_s (Craig & Banner 1994, Gerbi et al. 2009, Thomson et al. 2016), while surface waves additionally drive Langmuir turbulence through their associated Stokes drift (McWilliams et al. 1997). In this process, the interaction between the Stokes drift and the mean shear generates coherent Langmuir circulations that transport momentum and turbulence vertically, redistributing wave-generated energy deeper through the mixed layer. This coupling is represented using the vortex-force formalism (Craik & Leibovich 1976, McWilliams et al. 1997), which explicitly links surface wave kinematics to upper-ocean momentum balances. Through their influence on mixed-layer depth, SST, and near-surface stratification (Couvelard et al. 2020), these processes may provide an indirect pathway for modifying the potential energy of the coupled system and may interact with TFB by altering the background state on which buoyancy fluxes act.

The extent to which wave–wind controls on drag, wave–current controls on sea state heterogeneity, and wave-driven turbulence and dissipation contribute to the overall energy budget has not been systematically assessed within a unified energetic framework. For studies focused on TFB and CFB, this could be an important issue because waves can increase drag and KE extraction under opposing wave–current conditions and act as an additional influence by modifying stress and dissipation in ways not attributable to TFB and CFB.

6. THE FUTURE OF OBSERVATION AND MODELING

Future observational and modeling studies should focus on addressing several remaining gaps, which are summarized below.

6.1. Scale Sensitivity of Feedback Effects

Recent satellite missions such as SWOT are revolutionizing our ability to quantify not only the oceanic submesoscale activity but also the feedback of surface currents on wave fields (Villas Bôas et al. 2025) and the TFB effect on wind dynamics (Kaouah et al. 2025) that can induce an energization of submesoscale current (Renault et al. 2024b, 2025). As highlighted in Sections 2 and 3, modeling studies have revealed the scale dependence of both TFB and CFB mechanisms, as well as their interregional variability and nonlinear combined effects. To further advance these emerging research areas, two complementary strategies are essential:

- Future missions (such as Harmony; López-Dekker et al. 2021) and targeted in situ campaigns [including the Sub-Mesoscale Ocean Dynamics Experiment (S-MODE) (Farrar et al. 2025) and WHIRLS (Swart et al. 2023)] are designed to deepen our understanding of fine-scale air–sea interactions. By integrating coupled ocean–atmosphere measurements (e.g., wave characteristics), these efforts will also support the development of observation-based parameterizations. Additionally, future satellite missions should aim to coherently measure surface currents and surface stress, as originally proposed by the ODYSEA mission (Rodríguez et al. 2019).
- Sensitivity numerical experiments that isolate mesoscale TFB/CFB effects (Putrasahan et al. 2013, Seo et al. 2016, Renault et al. 2019b) are needed to disentangle their impacts.

Together, these synergistic approaches will not only refine our mechanistic understanding but also help bridge the gap between observational and modeling challenges in ocean–atmosphere interaction research.

6.2. Regions of Particular Interest

For offshore regions, at the mesoscale, TFB-induced wind anomalies are generally incoherent with ocean currents, leading to weak eddy wind work (Renault et al. 2017b). Tropical instability waves are a notable exception: In the eastern equatorial Pacific, SST anomalies drive wind responses coherently aligned with surface currents, producing significant negative eddy wind work (Seo et al. 2007, Holmes et al. 2024). In this regime, TFB and CFB reinforce the wind–current anticorrelation and enhance ocean KE extraction. Similar coupled behavior remains largely unidentified elsewhere, though the Southern Ocean may represent another sensitive regime where TFB/CFB interactions synergistically influence Antarctic Circumpolar Current energetics and eddy saturation.

For coastal regions, coastal and orographic effects can strongly modulate TFB and CFB. Interactions among winds, topography, and circulation affect nutrient delivery and productivity (Caldeira et al. 2005, Kessouri et al. 2022). In regions such as the Santa Barbara Channel, orography can energize submesoscales, counteracting eddy killing and altering nutrient supply.

Reanalyses often miss these fine-scale wind effects, highlighting the need for high-resolution coupled simulations.

6.3. Spatial Scales of Coupling and High Frequency

To determine the appropriate scale for considering the coupling between the ocean and the atmosphere, we recognize that mesoscale air–sea interactions significantly influence the ocean's energy budget and dynamics. Submesoscale interactions, though generally weaker, remain relevant. At very fine scales (<10 km), TFB may dominate, potentially causing a sink of potential energy from submesoscale currents to the atmosphere, thereby damping these currents (Renault et al. 2024b). Large eddy simulations (Sullivan et al. 2025) are essential for evaluating the importance of coupling at even smaller scales and developing scale-aware parameterizations. Recent observations from the S-MODE campaign (Farrar et al. 2025) have revealed wind rolls and associated oceanic responses at scales below 2 km, adding complexity that could mask or inhibit both TFB and CFB. However, our mechanistic understanding of air–sea interactions at small spatial and temporal scales remains incomplete, as discussed in Section 3. This gap is due to the nonlinear and transient dynamics characteristic of these scales and the high demands they place on observational and computational approaches. To enhance the quantification of air–sea interactions and their impacts on ocean energy, we must better consider interactions across different scales, such as those between IGWs and balanced motions. Additionally, addressing uncertainties related to air–sea fluxes and bulk formulas, as introduced by factors like the surface wave field (Section 5) and the transient nature of air–sea–wave interactions during severe storms or cold outbreaks, is crucial.

6.4. Toward a Coupled Ocean–Atmosphere Energetic Budget

Another important research line on the energetics of air–sea interactions aims to establish a coupled ocean–atmosphere energetic budget grounded in the Lorenz energy cycle. Building on recent advances, including the Gulf Stream analysis by Contreras et al. (2026), this framework seeks to identify the spatial and temporal scales at which mesoscale and submesoscale coupling becomes energetically significant for both fluids. It explicitly separates direct and indirect impacts of fine-scale coupling. Direct effects arise from wind responses to TFB and CFB. CFB induces wind anomalies of approximately 30% of the surface current amplitude (Renault et al. 2020), propagating up to the troposphere (Renault et al. 2016b), and provides an efficient pathway for KE transfer (wind work) from ocean to atmosphere. TFB can energize submesoscale motions and influence both KE and APE pathways.

6.5. Improving Atmospheric Boundary-Layer Models

A key area requiring substantial improvement in numerical models is the representation of the atmospheric boundary- and surface-layer processes, particularly within bulk flux formulations such as COARE that determine surface stress and wind response under TFB and CFB. Current atmospheric models rely on given atmospheric boundary- and surface-layer schemes to parameterize stress magnitude, direction, and stability dependence (Perlin et al. 2014, Samelson et al. 2024). These schemes generally assume an equilibrium sea state, simplified roughness relationships, and a steady-state boundary-layer adjustment—assumptions that are increasingly challenged by recent observations in dynamically active regions. As shown in this review, stress magnitude and direction can be modified by sea state, wave–current interaction, and current-relative winds, implying that errors in surface-layer parameterization may directly bias diagnosed wind work and coupled energetics. Improved in situ measurements and satellite remote sensing of wind stress, waves, and surface currents are therefore essential to significantly enhance our understanding of the response of wind and wind stress to environmental conditions (Desbiolles et al. 2023). Targeted observations in air–sea transition zones (Cronin et al. 2019, Clayson et al. 2023), combined with large eddy simulations and high-resolution regional modeling, could guide refinement of existing parameterizations and enable the development of more accurate models, potentially leveraging machine learning techniques trained on observations and high-fidelity process-resolving models.

6.6. Improving Uncoupled Ocean Models

For uncoupled ocean models, CFB parameterizations such as those developed by Renault et al. (2020) are based primarily on coupled models, but they are limited in terms of scale awareness [e.g., they are not valid at submesoscale (Renault et al. 2024b), may not be appropriate for high-frequency motions, and exhibit regional dependence (Renault et al. 2020, Conejero et al. 2024, Renault et al. 2024b)]. Satellite and in situ observational data could improve the accuracy of these parameterizations. In the longer term, a simplified atmospheric boundary-layer model (Lemarié et al. 2021) could be employed to represent both TFB and CFB. However, this type of model still needs to be rigorously evaluated in realistic configurations across both mesoscale and submesoscale regimes. In parallel, machine learning approaches trained on observational and high-resolution numerical datasets offer a promising alternative to more accurately predict wind stress and heat flux responses to TFB and CFB over a wide range of spatial scales.

6.7. High-Resolution Global Coupled Models and Upscaling

Air–sea coupling damps submesoscale currents and IGWs, impacting ocean mixing and the upscale transfer of KE to the mesoscale. These processes influence upper-ocean stratification, mixed-layer depth, and ultimately heat storage and large-scale turbulent fluxes. The cross-scale effects remain underquantified, highlighting the need for future research across different oceanic regions. Future research should focus on the impact of fine-scale air–sea interactions on climate modes. Evaluating the large-scale adjustment induced by fine-scale TFB and CFB in global coupled models is challenging and can be approached using two distinct strategies.

First, a direct comparison between an uncoupled ocean model and a fully coupled ocean–atmosphere model is generally not meaningful, because differences in the atmospheric mean state, forcing frequency, model resolution, and parameterizations can substantially influence the results. To isolate the specific contribution of TFB and CFB, the coupled and forced configurations must therefore be constructed to share, as closely as possible, the same large-scale atmospheric state and forcing characteristics (see, e.g., figure 11 in Renault et al. 2020).

A second approach to assess upscaling effects involves smoothing the ocean fields perceived by the atmosphere so that only certain scales are transmitted to the atmospheric model, effectively suppressing fine-scale coupling pathways (Seo et al. 2016, Renault et al. 2019b). Such experimental designs are crucial for attributing observed large-scale adjustments specifically to fine-scale TFB and CFB rather than to structural differences between models.

SUMMARY POINTS

1. The ocean's energy cycle is driven by complex interactions between wind, Earth's rotation, topography, and eddies at the mesoscale and submesoscale. Current feedback (CFB) extracts kinetic energy (KE) from mesoscale eddies, while thermal feedback (TFB)

depletes potential energy, weakening baroclinic instability. However, their combined impact on the ocean's energy budget remains partially uncertain.

2. Submesoscale eddies and internal gravity waves (IGWs) play a key role in the ocean's forward energy cascade. Submesoscale eddy killing linked to CFB is more effective at damping eddies than at the mesoscale, but its overall impact is constrained by the short lifetime of submesoscale eddies. IGWs are strongly damped by CFB; however, quantitative uncertainty about the coupled air–sea response remains. TFB reduces upper-ocean available potential energy (APE), indirectly damping KE. The energetic consequences of these processes, especially considering cross-scale fluxes, are still not fully understood.
3. Mesoscale air–sea interactions stabilize major ocean currents (e.g., the Gulf Stream and Agulhas Current), reducing meandering and altering large-scale sea surface temperature patterns. These changes affect the APE available in the atmosphere—both locally and remotely through planetary waves—with consequences for storm tracks and intensity, and likely for climate variability. Submesoscale processes and waves may further modulate this upscaling effect.
4. Surface gravity waves introduce critical heterogeneity in momentum flux and near-surface dissipation. Their interactions with wind and currents may amplify or weaken TFB and CFB, but a better quantification of their long-term climatological impacts is needed, especially in dynamic regions like western boundary currents.

DISCLOSURE STATEMENT

The authors are not aware of any affiliations, memberships, funding, or financial holdings that might be perceived as affecting the objectivity of this review.

ACKNOWLEDGMENTS

L.R. acknowledges support from the CNES TOSCA SWOT-Poseidon and M-ODYSEA projects, as well as the Shom PROTEVSII project. This work used the GENCI (project 13051) computing resources. J.O.W. was supported by the US National Science Foundation under grant OCE-2524894. H.S. acknowledges support from the US National Science Foundation (OCE-2148120), NASA (80NSSC21K1524), the Office of Naval Research (N000142412570 and N000142612046), and the Uehiro Center for the Advancement of Oceanography at the University of Hawai'i at Mānoa. We appreciate fruitful discussions with S. Masson as well as input from A. Thompson, I. Uchoa, and G. Marechal.

LITERATURE CITED

Alford MH. 2020. Revisiting near-inertial wind work: slab models, relative stress, and mixed layer deepening. *J. Phys. Oceanogr.* 50(11):3141–56

Alford MH, MacKinnon JA, Simmons HL, Nash JD. 2016. Near-inertial internal gravity waves in the ocean. *Annu. Rev. Mar. Sci.* 8:95–123

Ardhuin F, Gille ST, Menemenlis D, Rocha CB, Rascle N, et al. 2017. Small-scale open ocean currents have large effects on wind wave heights. *J. Geophys. Res. Oceans* 122(6):4500–17

Bai Y, Thompson AF, Villas Bôas AB, Klein P, Torres HS, Menemenlis D. 2023. Sub-mesoscale wind-front interactions: the combined impact of thermal and current feedback. *Geophys. Res. Lett.* 50(18):e2023GL104807

Barkan R, Srinivasan K, McWilliams JC. 2024. Eddy–internal wave interactions: stimulated cascades in cross-scale kinetic energy and enstrophy fluxes. *J. Phys. Oceanogr.* 54(6):1309–26

Barkan R, Winters KB, Smith SGL. 2015. Energy cascades and loss of balance in a reentrant channel forced by wind stress and buoyancy fluxes. *J. Phys. Oceanogr.* 45(1):272–93

Bentamy A, Croize-Fillon D, Perigaud C. 2008. Characterization of ASCAT measurements based on buoy and QuikSCAT wind vector observations. *Ocean Sci.* 4(4):265–74

Bishop SP, Small RJ, Bryan FO. 2020. The global sink of available potential energy by mesoscale air-sea interaction. *J. Adv. Model. Earth Syst.* 12(10):e2020MS002118

Bretherton FP, Garrett CJR. 1968. Wavetrains in inhomogeneous moving media. *Proc. R. Soc. A* 302(1471):529–54

Bühler O, McIntyre ME. 2005. Wave capture and wave–vortex duality. *J. Fluid Mech.* 534:67–95

Buijsman MC, Abdulfatai M, Arbic BK, Chassignet EP, Hiron L, et al. 2025. Energetics of (super)tidal baroclinic modes in a realistically forced global ocean simulation. *J. Geophys. Res. Oceans* 130(6):e2025JC022460

Bye JAT. 1985. Large-scale momentum exchange in the coupled atmosphere-ocean. In *Coupled Ocean-Atmosphere Models*, ed. JCJ Nihoul. Elsevier Oceanography Series Vol. 40. Elsevier

Caldeira RM, Marchesiello P, Nezlin NP, DiGiacomo PM, McWilliams JC. 2005. Island wakes in the southern California Bight. *J. Geophys. Res. Oceans* 110(C11):C11012

Capet X, McWilliams JC, Molemaker MJ, Shchepetkin AF. 2008a. Mesoscale to submesoscale transition in the California Current System. Part I: flow structure, eddy flux, and observational tests. *J. Phys. Oceanogr.* 38(1):29–43

Capet X, McWilliams JC, Molemaker MJ, Shchepetkin AF. 2008b. Mesoscale to submesoscale transition in the California Current System. Part II: frontal processes. *J. Phys. Oceanogr.* 38(1):44–64

Chassignet EP, Xu X. 2021. On the importance of high-resolution in large-scale ocean models. *Adv. Atmos. Sci.* 38(10):1621–34

Chawla A, Kirby JT. 2002. Monochromatic and random wave breaking at blocking points. *J. Geophys. Res. Oceans* 107(C7):4-1–19

DB Chelton, Schlax MG, Freilich MH, Milliff RF. 2004. Satellite measurements reveal persistent small-scale features in ocean winds. *Science* 303(5660):978–83

Chen SS, Zhao W, Donelan MA, Tolman HL. 2013. Directional wind–wave coupling in fully coupled atmosphere–wave–ocean models: results from CBLAST-Hurricane. *J. Atmos. Sci.* 70(10):3198–215

Cho A, Song H, Seo H, Sun R, Mazloff MR, et al. 2025. Dynamic and thermodynamic coupling between the atmosphere and ocean near the Kuroshio current and extension system. *Ocean Model.* 194:102496

Clayson CA, Demott CA, de Szoeke SP, Chang P, Foltz GR, et al. 2023. *A new paradigm for observing and modeling of air-sea interactions to advance Earth system prediction*. Rep., US CLIVAR Project Office

Conejero C, Renault L, Desbiolles F, McWilliams J, Giordani H. 2024. Near-surface atmospheric response to meso- and submesoscale current and thermal feedbacks. *J. Phys. Oceanogr.* 54(3):823–48

Contreras M, Marchesiello P, Renault L. 2026. Submesoscale energy cycle in a coupled ocean-atmosphere simulation of the Gulf Stream. *Geophys. Res. Lett.* 53(8):e2025GL119360

Contreras M, Renault L, Marchesiello P. 2023. Understanding energy pathways in the Gulf Stream. *J. Phys. Oceanogr.* 53(3):719–36

Couvelard X, Lemarié F, Samson G, Redelsperger JL, Ardhuin F, et al. 2020. Development of a two-way-coupled ocean–wave model: assessment on a global NEMO (v3.6)–WW3 (v6.02) coupled configuration. *Geosci. Model Dev.* 13(7):3067–90

Craig PD, Banner ML. 1994. Modeling wave-enhanced turbulence in the ocean surface layer. *J. Phys. Oceanogr.* 24(12):2546–59

Craik AD, Leibovich S. 1976. A rational model for Langmuir circulations. *J. Fluid Mech.* 73(3):401–26

Cronin MF, Gentemann CL, Edson J, Ueki I, Bourassa M, et al. 2019. Air-sea fluxes with a focus on heat and momentum. *Front. Mar. Sci.* 6:430

Csanady GT, Gibson M. 2001. *Air-Sea Interaction: Laws and Mechanisms*. Cambridge University Press

D'Asaro E, Lee C, Rainville L, Harcourt R, Thomas L. 2011. Enhanced turbulence and energy dissipation at ocean fronts. *Science* 332(6027):318–22

Debreu L, Kevlahan NR, Marchesiello P. 2022. Improved Gulf Stream separation through Brinkman penalization. *Ocean Model.* 179:102121

Delpech A, Barkan R, Renault L, McWilliams J, Siyanbola OQ, et al. 2023. Wind-current feedback is an energy sink for oceanic internal waves. *Sci. Rep.* 13(1):5915

Desbiolles F, Meroni AN, Renault L, Pasquero C. 2023. Environmental control of wind response to sea surface temperature patterns in reanalysis dataset. *J. Clim.* 36(12):3881–93

Donelan MA. 1990. Air-sea interaction. In *The Sea*, Vol. 9, Part A: *Ocean Engineering Science*, ed. B Le Mehaute, DM Hanes. Wiley

Dong J, Fox-Kemper B, Wenegrat JO, Bodner AS, Yu X, et al. 2024. Submesoscales are a significant turbulence source in global ocean surface boundary layer. *Nat. Commun.* 15(1):9566

Ducet N, Le Traon PY, Reverdin G. 2000. Global high-resolution mapping of ocean circulation from TOPEX/Poseidon and ERS-1 and-2. *J. Geophys. Res. Oceans* 105(C8):19477–98

Edson JB, Jampana V, Weller RA, Bigorre SP, Plueddemann AJ, et al. 2013. On the exchange of momentum over the open ocean. *J. Phys. Oceanogr.* 43(8):1589–610

Farrar JT, D'Asaro E, Rodríguez E, Shcherbina A, Lenain L, et al. 2025. S-MODE: the Sub-Mesoscale Ocean Dynamics Experiment. *Bull. Am. Meteorol. Soc.* 106(4):E657–77

Flexas MM, Thompson AF, Torres HS, Klein P, Farrar JT, et al. 2019. Global estimates of the energy transfer from the wind to the ocean, with emphasis on near-inertial oscillations. *J. Geophys. Res. Oceans* 124(8):5723–46

Garabato ACN, Yu X, Callies J, Barkan R, Polzin KL, et al. 2022. Kinetic energy transfers between mesoscale and submesoscale motions in the open ocean's upper layers. *J. Phys. Oceanogr.* 52(1):75–97

Gerbi GP, Trowbridge JH, Terray EA, Plueddemann AJ, Kukulka T. 2009. Observations of turbulence in the ocean surface boundary layer: energetics and transport. *J. Phys. Oceanogr.* 39(5):1077–96

Gille ST, Ardhuin F, Villa Bôas AB. 2025. Wind, waves, and surface currents: interactions at mesoscales and submesoscales. *Annu. Rev. Mar. Sci.* 18:65–88

Holmes RM, Renault L, Maillard L, Boucharel J. 2024. Air–sea coupling feedbacks over tropical instability waves. *J. Phys. Oceanogr.* 54(10):2165–84

Husain NT, Hara T, Sullivan PP. 2022. Wind turbulence over misaligned surface waves and air–sea momentum flux. Part I: waves following and opposing wind. *J. Phys. Oceanogr.* 52(1):119–39

Iyer S, Drushka K, Thompson EJ, Thomson J. 2022a. Small-scale spatial variations of air-sea heat, moisture, and buoyancy fluxes in the tropical trade winds. *J. Geophys. Res. Oceans* 127(10):e2022JC018972

Iyer S, Thomson J, Thompson E, Drushka K. 2022b. Variations in wave slope and momentum flux from wave-current interactions in the tropical trade winds. *J. Geophys. Res. Oceans* 127(3):e2021JC018003

Jullien S, Masson S, Oerder V, Samson G, Colas F, Renault L. 2020. Impact of ocean–atmosphere current feedback on ocean mesoscale activity: regional variations and sensitivity to model resolution. *J. Clim.* 33(7):2585–602

Kaouah M, Lapeyre G, Renault L, Perrot X, Dablemont C. 2025. Submesoscale air-sea interactions as revealed by SWOT. *Geophys. Res. Lett.* 52(20):e2025GL116017

Kessouri F, Renault L, McWilliams JC, Damien P, Bianchi D. 2022. Enhancement of oceanic eddy activity by fine-scale orographic winds drives high productivity, low oxygen, and low pH conditions in the Santa Barbara Channel. *J. Geophys. Res. Oceans* 127(12):e2022JC018947

Klein P, Hua BL, Lapeyre G, Capet X, Le Gentil S, Sasaki H. 2008. Upper ocean turbulence from high-resolution 3D simulations. *J. Phys. Oceanogr.* 38(8):1748–63

Klein P, Lapeyre G, Siegelman L, Qiu B, Fu LL, et al. 2019. Ocean-scale interactions from space. *Earth Space Sci.* 6(5):795–817

Kwak K, Song H, Marshall J, Seo H, McGillicuddy DJ Jr. 2021. Suppressed $p\mathrm{CO}_2$ in the Southern Ocean due to the interaction between current and wind. *J. Geophys. Res. Oceans* 126(12):e2021JC017884

LaCasce J. 2012. Surface quasigeostrophic solutions and baroclinic modes with exponential stratification. *J. Phys. Oceanogr.* 42(4):569–80

Larrañaga M, Renault L, Jouanno J. 2022. Partial control of the Gulf of Mexico dynamics by the current feedback to the atmosphere. *J. Phys. Oceanogr.* 52(10):2515–30

Larrañaga M, Renault L, Wineteer A, Contreras M, Arbic BK, et al. 2025. Assessing the future ODYSEA satellite mission for the estimation of ocean surface currents, wind stress, energy fluxes, and the mechanical coupling between the ocean and the atmosphere. *Remote Sens.* 17(2):302

Lemarié F, Samson G, Redelsperger JL, Giordani H, Brivoal T, Madec G. 2021. A simplified atmospheric boundary layer model for an improved representation of air-sea interactions in eddying oceanic models: implementation and first evaluation in NEMO (4.0). *Geosci. Model Dev.* 14:543–72

Liu Y, Jing Z, Wu L. 2019. Wind power on oceanic near-inertial oscillations in the global ocean estimated from surface drifters. *Geophys. Res. Lett.* 46(5):2647–53

López-Dekker P, Biggs J, Chapron B, Hooper A, Kääb A, et al. 2021. The Harmony mission: end of phase-0 science overview. In *2021 IEEE International Geoscience and Remote Sensing Symposium (IGARSS)*. IEEE

Luo JJ, Masson S, Roeckner E, Madec G, Yamagata T. 2005. Reducing climatology bias in an ocean–atmosphere CGCM with improved coupling physics. *J. Clim.* 18(13):2344–60

Ma X, Jing Z, Chang P, Liu X, Montuoro R, et al. 2016. Western boundary currents regulated by interaction between ocean eddies and the atmosphere. *Nature* 535(7613):533–37

Marchesiello P, Capet X, Menkes C, Kennan SC. 2011. Submesoscale dynamics in tropical instability waves. *Ocean Model.* 39(1):31–46

Marchesiello P, McWilliams JC, Shchepetkin A. 2003. Equilibrium structure and dynamics of the California Current System. *J. Phys. Oceanogr.* 33(4):753–83

Marechal G, de Marez C. 2022. Variability of surface gravity wave field over a realistic cyclonic eddy. *Ocean Sci.* 18(5):1275–92

McGillicuddy DJ Jr. 2015. Formation of intrathermocline lenses by eddy–wind interaction. *J. Phys. Oceanogr.* 45(2):606–12

McGillicuddy DJ Jr., Anderson LA, Bates NR, Bibby T, Buesseler KO, et al. 2007. Eddy/wind interactions stimulate extraordinary mid-ocean plankton blooms. *Science* 316(5827):1021–26

McWilliams JC. 2016. Submesoscale currents in the ocean. *Proc. R. Soc. A* 472(2189):20160117

McWilliams JC, Sullivan PP, Moeng CH. 1997. Langmuir turbulence in the ocean. *J. Fluid Mech.* 334:1–30

Molemaker MJ, McWilliams JC. 2010. Local balance and cross-scale flux of available potential energy. *J. Fluid Mech.* 645:295–314

Nuijens L, Wenegrat JO, Lopez Dekker P, Pasquero C, O'Neill LW, et al. 2024. *The air-sea interaction (ASI) submesoscale: physics and impact*. White Paper, Lorentz Center Workshop

Ortiz-Suslow DG, Laxague N, Björkqvist JV, Curcic M. 2025. Accounting for ocean waves and current shear in wind stress parameterization. *Bound.-Layer Meteorol.* 191(9):38

Özgökmen TM, Chassignet EP. 2002. Dynamics of two-dimensional turbulent bottom gravity currents. *J. Phys. Oceanogr.* 32(5):1460–78

Patton EG, Sullivan PP, Kosović B, Dudhia J, Mahrt L, et al. 2019. On the influence of swell propagation angle on surface drag. *J. Appl. Meteorol. Climatol.* 58(5):1039–59

Perlin N, de Szoeke SP, Chelton DB, Samelson RM, Skyllingstad ED, O'Neill LW. 2014. Modeling the atmospheric boundary layer wind response to mesoscale sea surface temperature perturbations. *Mon. Weather Rev.* 142(11):4284–307

Phillips OM. 1966. *The Dynamics of the Upper Ocean*. Cambridge University Press

Phillips OM. 1985. Spectral and statistical properties of the equilibrium range in wind-generated gravity waves. *J. Fluid Mech.* 156:505–31

Porchetta S, Temel O, Warner J, Muñoz-Esparza D, Monbaliu J, et al. 2021. Evaluation of a roughness length parametrization accounting for wind–wave alignment in a coupled atmosphere–wave model. *Q. J. R. Meteorol. Soc.* 147(735):825–46

Putrasahan DA, Miller AJ, Seo H. 2013. Regional coupled ocean–atmosphere downscaling in the Southeast Pacific: impacts on upwelling, mesoscale air–sea fluxes, and ocean eddies. *Ocean Dyn.* 63(5):463–88

Qiu B, Chen S, Klein P, Sasaki H, Sasai Y. 2014. Seasonal mesoscale and submesoscale eddy variability along the North Pacific Subtropical Countercurrent. *J. Phys. Oceanogr.* 44(12):3079–98

Rai S, Hecht M, Maltrud M, Aluie H. 2021. Scale of oceanic eddy killing by wind from global satellite observations. *Sci. Adv.* 7(28):eabf4920

Raj A, Kumar BP, Jampana V, Remya PG, Seo H, et al. 2025. Wind-stress misalignment in the presence of swells in the Bay of Bengal. *Front. Mar. Sci.* 12:1647849

Rath W, Greatbatch RJ, Zhai X. 2013. Reduction of near-inertial energy through the dependence of wind stress on the ocean-surface velocity. *J. Geophys. Res. Oceans* 118(6):2761–73

Renault L, Arsouze T, Desbiolles F, Small J. 2024a. Rectification effects of regional air–sea interactions over western boundary current on large-scale sea surface temperature and extra-tropical storm tracks. *Sci. Rep.* 14(1):31771

Renault L, Conejero C, Wenegrat J, Uchoa I. 2025. Interplay of submesoscale current and thermal feedbacks: a seasonal perspective in the Gulf Stream. *Geophys. Res. Lett.* 52(21):e2025GL116960

Renault L, Contreras M, Marchesiello P, Conejero C, Uchoa I, Wenegrat J. 2024b. Unraveling the impacts of submesoscale thermal and current feedbacks on the low-level winds and oceanic submesoscale currents. *J. Phys. Oceanogr.* 54(12):2463–86

Renault L, Marchesiello P. 2022. Ocean tides can drag the atmosphere and cause tidal winds over broad continental shelves. *Commun. Earth Environ.* 3(1):70

Renault L, Marchesiello P, Contreras M. 2023a. Coaction of top and bottom drags in Gulf Stream dynamics. *J. Geophys. Res. Oceans* 128(3):e2022JC018939

Renault L, Marchesiello P, Masson S, McWilliams JC. 2019a. Remarkable control of Western Boundary Currents by eddy killing, a mechanical air-sea coupling process. *Geophys. Res. Lett.* 46(5):2743–51

Renault L, Masson S, Arsouze T, Madec G, McWilliams JC. 2020. Recipes for how to force oceanic model dynamics. *J. Adv. Model. Earth Syst.* 12(2):e2019MS001715

Renault L, Masson S, Oerder V, Colas F, McWilliams J. 2023b. Modulation of the oceanic mesoscale activity by the mesoscale thermal feedback to the atmosphere. *J. Phys. Oceanogr.* 53(7):1651–67

Renault L, Masson S, Oerder V, Jullien S, Colas F. 2019b. Disentangling the mesoscale ocean-atmosphere interactions. *J. Geophys. Res. Oceans* 124(3):2164–78

Renault L, McWilliams JC, Gula J. 2018. Dampening of submesoscale currents by air-sea stress coupling in the Californian upwelling system. *Sci. Rep.* 8(1):13388

Renault L, McWilliams JC, Masson S. 2017a. Satellite observations of imprint of oceanic current on wind stress by air-sea coupling. *Sci. Rep.* 7(1):17747

Renault L, McWilliams JC, Penven P. 2017b. Modulation of the Agulhas Current retroflection and leakage by oceanic current interaction with the atmosphere in coupled simulations. *J. Phys. Oceanogr.* 47(8):2077–100

Renault L, Molemaker MJ, Gula J, Masson S, McWilliams JC. 2016a. Control and stabilization of the Gulf Stream by oceanic current interaction with the atmosphere. *J. Phys. Oceanogr.* 46(11):3439–53

Renault L, Molemaker MJ, McWilliams JC, Shchepetkin AF, Lemarié F, et al. 2016b. Modulation of wind work by oceanic current interaction with the atmosphere. *J. Phys. Oceanogr.* 46(6):1685–704

Reynolds RW, Smith TM, Liu C, Chelton DB, Casey KS, Schlax MG. 2007. Daily high-resolution-blended analyses for sea surface temperature. *J. Clim.* 20(22):5473–96

Rodríguez E, Bourassa M, Chelton D, Farrar JT, Long D, et al. 2019. The Winds and Currents Mission concept. *Front. Mar. Sci.* 6:438

Samelson R, Durski S, Chelton D, Skyllingstad E, Barbour P. 2024. Surface currents and relative-wind stress in coupled ocean–atmosphere simulations of the Northern California Current System. *Mon. Weather Rev.* 152(9):2033–54

Sauvage C, Seo H, Barr BW, Edson JB, Clayson CA. 2024. Misaligned wind-waves behind atmospheric cold fronts. *J. Geophys. Res. Oceans* 129(9):e2024JC021162

Sauvage C, Seo H, Clayson CA, Edson JB. 2023. Improving wave-based air-sea momentum flux parameterization in mixed seas. *J. Geophys. Res. Oceans* 128(3):e2022JC019277

Schmidtko S, Johnson GC, Lyman JM. 2013. MIMOC: a global monthly isopycnal upper-ocean climatology with mixed layers. *J. Geophys. Res. Oceans* 118(4):1658–72

Schoonover J, Dewar W, Wienders N, Gula J, McWilliams JC, et al. 2016. North Atlantic barotropic vorticity balances in numerical models. *J. Phys. Oceanogr.* 46(1):289–303

Schubert R, Gula J, Greatbatch RJ, Baschek B, Biastoch A. 2020. The submesoscale kinetic energy cascade: mesoscale absorption of submesoscale mixed layer eddies and frontal downscale fluxes. *J. Phys. Oceanogr.* 50(9):2573–89

Scott RB, Xu Y. 2009. An update on the wind power input to the surface geostrophic flow of the world ocean. *Deep-Sea Res. I* 56(3):295–304

Seo H. 2017. Distinct influence of air–sea interactions mediated by mesoscale sea surface temperature and surface current in the Arabian Sea. *J. Clim.* 30(20):8061–80

Seo H, Jochum M, Murtugudde R, Miller AJ, Roads JO. 2007. Feedback of tropical instability-wave-induced atmospheric variability onto the ocean. *J. Clim.* 20(23):5842–55

Seo H, Miller AJ, Norris JR. 2016. Eddy–wind interaction in the California Current System: dynamics and impacts. *J. Phys. Oceanogr.* 46(2):439–59

Seo H, O'Neill LW, Bourassa MA, Czaja A, Drushka K, et al. 2023. Ocean mesoscale and frontal-scale ocean–atmosphere interactions and influence on large-scale climate: a review. *J. Clim.* 36(7):1981–2013

Seo H, Song H, O'Neill LW, Mazloff MR, Cornuelle BD. 2021. Impacts of ocean currents on the South Indian Ocean extratropical storm track through the relative wind effect. *J. Clim.* 34(22):9093–113

Seo H, Subramanian AC, Song H, Chowdary JS. 2019. Coupled effects of ocean current on wind stress in the Bay of Bengal: Eddy energetics and upper ocean stratification. *Deep-Sea Res. II* 168:104617

Shao M, Wu L. 2024. Atmospheric fronts shaping the (sub) mesoscale SST-wind coupling over the southern ocean: observational case. *J. Geophys. Res. Atmos.* 129(8):e2023JD039386

Skyllingstad ED, Vickers D, Mahrt L, Samelson R. 2007. Effects of mesoscale sea-surface temperature fronts on the marine atmospheric boundary layer. *Bound.-Layer Meteorol.* 123:219–37

Small RJ, de Szoeke SP, Xie S, O'Neill L, Seo H, et al. 2008. Air–sea interaction over ocean fronts and eddies. *Dyn. Atmos. Oceans* 45(3–4):274–319

Song H, Marshall J, McGillicuddy DJ Jr., Seo H. 2020. Impact of current-wind interaction on vertical processes in the southern ocean. *J. Geophys. Res. Oceans* 125(4):e2020JC016046

Srinivasan K, Barkan R, McWilliams JC. 2023. A forward energy flux at submesoscales driven by frontogenesis. *J. Phys. Oceanogr.* 53(1):287–305

Su Z, Wang J, Klein P, Thompson AF, Menemenlis D. 2018. Ocean submesoscales as a key component of the global heat budget. *Nat. Commun.* 9(1):775

Sullivan PP, Banner ML, Morison RP, Peirson WL. 2018. Turbulent flow over steep steady and unsteady waves under strong wind forcing. *J. Phys. Oceanogr.* 48(1):3–27

Sullivan PP, McWilliams JC, Patton EG. 2025. An investigation of coupled atmospheric and oceanic boundary layers using large-eddy simulation. *J. Atmos. Sci.* 82(4):829–46

Sullivan PP, McWilliams JC, Weil JC, Patton EG, Fernando HJ. 2020. Marine boundary layers above heterogeneous SST: across-front winds. *J. Atmos. Sci.* 77(12):4251–75

Sverdrup HU. 1947. Wind-driven currents in a baroclinic ocean; with application to the equatorial currents of the Eastern Pacific. *PNAS* 33(11):318–26

Swart S, du Plessis MD, Nicholson SA, Monteiro P, Dove LA, et al. 2023. The Southern Ocean mixed layer and its boundary fluxes: fine-scale observational progress and future research priorities. *Philos. Trans. R. Soc. A* 381(2249):20220058

Taylor JR, Ferrari R. 2010. Buoyancy and wind-driven convection at mixed layer density fronts. *J. Phys. Oceanogr.* 40(6):1222–42

Taylor JR, Thompson AF. 2023. Submesoscale dynamics in the upper ocean. *Annu. Rev. Fluid Mech.* 55:103–27

Tedesco P, Gula J, Penven P, Ménesguen C, Jamet Q, Vic C. 2024. Can mesoscale eddy kinetic energy sources and sinks be inferred from sea surface height in the Agulhas Current region? *J. Geophys. Res. Oceans* 129(4):e2023JC020833

Thomas J, Daniel D. 2021. Forward flux and enhanced dissipation of geostrophic balanced energy. *J. Fluid Mech.* 911:A60

Thomas LN. 2012. On the effects of frontogenetic strain on symmetric instability and inertia–gravity waves. *J. Fluid Mech.* 711:620–40

Thomson J, D'Asaro EA, Cronin MF, Rogers WE, Harcourt RR, Shcherbina A. 2013. Waves and the equilibrium range at Ocean Weather Station P: waves at Station P. *J. Geophys. Res. Oceans* 118(11):5951–62

Thomson J, Schwendeman MS, Zippel SF, Moghimi S, Gemmrich J, Rogers WE. 2016. Wave-breaking turbulence in the ocean surface layer. *J. Phys. Oceanogr.* 46(6):1857–70

Tomita H, Hihara T, Kako S, Kubota M, Kutsuwada K. 2019. An introduction to J-OFURO3, a third-generation Japanese ocean flux data set using remote-sensing observations. *J. Oceanogr.* 75(2):171–94

Torres HS, Klein P, D'Asaro E, Wang J, Thompson AF, et al. 2022a. Separating energetic internal gravity waves and small-scale frontal dynamics. *Geophys. Res. Lett.* 49(6):e2021GL096249

Torres HS, Klein P, Wang J, Wineteer A, Qiu B, et al. 2022b. Wind work at the air-sea interface: a modeling study in anticipation of future space missions. *Geosci. Model Dev.* 15(21):8041–58

Uchoa I, Wenegrat J, Renault L. 2025. Sink of eddy energy by submesoscale sea surface temperature variability in a coupled regional model. *J. Phys. Oceanogr.* 55(8):993–1007

Villas Bôas AB, Cornuelle BD, Mazloff MR, Gille ST, Ardhuin F. 2020. Wave–current interactions at meso- and submesoscales: insights from idealized numerical simulations. *J. Phys. Oceanogr.* 50(12):3483–500

Villas Bôas AB, Marechal G, Bohé A. 2025. Observing interactions between waves, winds, and currents from SWOT. *Geophys. Res. Lett.* 52(17):e2024GL114331

VreĆica T, Pizzo N, Lenain L. 2022. Observations of strongly modulated surface wave and wave breaking statistics at a submesoscale front. *J. Phys. Oceanogr.* 52(2):289–304

Wang H, Villa Bôas AB, Vanneste J, Young WR. 2025. Scattering of surface waves by ocean currents: the U2H map. *J. Fluid Mech.* 1005:A12

Wang H, Villas Bôas AB, Young WR, Vanneste J. 2023. Scattering of swell by currents. *J. Fluid Mech.* 975:A1

Wenegrat JO. 2023. The current feedback on stress modifies the Ekman buoyancy flux at fronts. *J. Phys. Oceanogr.* 53(12):2737–49

Wenegrat JO, Arthur R. 2018. Response of the atmospheric boundary layer to submesoscale sea surface temperature fronts. *Geophys. Res. Lett.* 45(24):13–505

Wineteer A, Rodriguez E, Martin DP, Torres H, Polverari F, et al. 2024. Exploring the characteristics of ocean surface winds at high resolution with Doppler scatterometry. *Geophys. Res. Lett.* 51(23):e2024GL113455

Xie SP. 2004. Satellite observations of cool ocean–atmosphere interaction. *Bull. Am. Meteorol. Soc.* 85(2):195–208

Zhai X. 2017. Dependence of energy flux from the wind to surface inertial currents on the scale of atmospheric motions. *J. Phys. Oceanogr.* 47(11):2711–19

Zhang L, Liu G, He Y, Perrie W. 2021. Impacts of momentum fluxes modulated by surface waves on near-inertial motions in tropical cyclones. *J. Geophys. Res. Oceans* 126(12):e2021JC017795

Zheng Z, Wenegrat JO, Fox-Kemper B, Brett GJ. 2025. Wind-catalyzed energy exchanges between fronts and boundary layer turbulence. *J. Phys. Oceanogr.* 55(9):1591–606